



# PROSTHETIC HAND SZCZYBURA FILIP

// PREPARED FOR SERVICE ROBOTS PROJECT



AKADEMIA GÓRNICZO-HUTNICZA  
IM. STANISŁAWA STASZICA  
W KRAKOWIE

2019-2020 // IMIR MECHATRONICS ENGINEERING

PROSTHETIC HAND  
**SZCZYBURA FILIP**

## Table of **contents**

1. INTRODUCTION PAGE.02
2. PROSTHETICS IN SPORTS PAGE.03
3. THE ROLE OF THE THUMB IN ANTOPOMORPHIC GRASPING PAGE.05
4. HUMAN HAND KINEMATIC SCHEME PAGE.09
5. HUMAN HAND PROSTHESIS - MODEL'S KINEMATIC SCHEME PAGE.10
6. DENAVIT-HARTENBERG NOTATION PAGE.12
7. FORWARD KINEMATICS PAGE.13
8. INVERSE KINEMATICS PAGE.18
9. MATERIAL SELECTION PAGE.20
10. MODEL VISUALISATION PAGE.26





My idea is to design a  
prosthetic hand  
**FOR PHYSICAL  
ACTIVITY TASKS**

// PREPARED FOR SERVICE ROBOTS PROJECT

## SERVICE ROBOTS PROSTHETIC HAND

There are so many patients who are disable in hand after going through accidents or sustained neurological damage. In the United States, approximately 500,000 people (171 per 100,000) experience a stroke each year. This high stroke incidence, in combination with an aging population, which implies future increases in incidence, greatly strains national healthcare services and related costs. In the majority of these cases, patients experience either partial or total absence of hand motion ability, and this loss of functionality can greatly restrict activities of daily living and considerably reduce quality of life. High intensity and task specific upper limb treatment consisting of active, highly repetitive movements is one of the most effective approaches to arm and hand function restoration. Unfortunately, standard multidisciplinary stroke rehabilitation is labor intensive and requires one-to-one manual interactions with therapists. Treatment protocols entail daily therapy for several weeks, which makes the provision of highly intensive treatment for all patients difficult. Therefore, a mechanic is required to support this work automatically.

The service robots may be defined as robots, which perform useful tasks characteristic for humanoid and other types of creatures, that are able to perform mechanical operations either static or dynamic. An intelligent prosthetic hand is defined as a hand that mimics the natural movements of the human hand. In order to appropriately mimic the motion of the human hand, its natural motions must be studied carefully. For instance, the distal phalanx (fingertip) must rotate about its joint as the middle phalanx rotates. There are some papers also described the method to make it. However, it is very difficult and unnatural to bend the finger at the proximal joint, while keeping the distal joint stiff. The motions of these two joints are linked and must move together. On the other hand, the knuckle joint is not linked to any other joints. The knuckle is able to move the entire finger with no motion in the proximal or distal joints.

The unique musculoskeletal structure of the human hand brings in wider dexterous capabilities to grasp and manipulate a repertoire of objects than the non-human primates. It has been widely accepted that the orientation and the position of the thumb plays an important role in this characteristic behavior. There have been numerous attempts to develop anthropomorphic robotic hands with varying levels of success. Nevertheless, manipulation ability in those hands is to be ameliorated even though they can grasp objects successfully. An appropriate model of the thumb is important to manipulate the objects against the fingers and to maintain the stability. Modeling these complex interactions about the mechanical axes of the joints and how to incorporate these joints in robotic thumbs is a challenging task.



# Controversy of THE PROSTHETICS in sports

PROSTHETICS ARE USED TO PERFORM THE TASKS OF THE PREVIOUSLY WORKING BODY PARTS , HOWEVER...

The worlds of sports and prosthetics are colliding, resulting in a realm of advanced prosthetics that has catapulted athletes into an era of revolutionary gains.

In the past few decades, the world of sports prosthetics for athletes has realized technological advancements that have allowed artificial body parts to become increasingly refined and targeted for high-level competition. From the rudimentary attempts at large-movement limbs through early research in the field to the pinpoint accuracy of advanced prosthetics for eyes, fingers and more, these modern innovations are making rivals out of the machines seen in sci-fi movies. Advanced sports prosthetics are enabling today's top athletes to not only participate in their chosen sport, but to excel on an international level as well.

Utilizing prosthetics for sports athletes to allow amputees to engage in their favorite sports is not a new concept. The combination of technology and cutting edge materials, however, has pushed the industry beyond simply allowing these athletes to enjoy their chosen sport. Athletes like Olympic track trailblazer Oscar Pistorius and X Games pro Mike Schultz are making history every time they compete, and are now passing the torch.

## Blades

These intricately curved lower-extremity prosthetics are arguably the most advanced and well-known sports prosthetics currently in use thanks to South African track and field superstar Oscar Pistorius. During his iconic appearance in the 2012 London Olympics as the first double leg amputee competing against able-bodied athletes, the 'Blade Runner,' as Pistorius is known, wore specially designed blades that allowed him to sprint at high speeds .Made of carbon fiber optimized using computer analysis and mechanical testing, these blades are specially fabricated to match the runner's weight and impact level while providing the appropriate amount of traction. The original Flex-Foot blades worn by Pistorius were designed by Francois Van Der Watt who now practices at Horton's Orthotics & Prosthetics in Fort Smith and has since worked with many other Paralympic athletes around the world.

## Moto Knee & Versa Foot

After losing his leg in a snowmobile accident, X Games snowmobile and motocross racer Mike Schultz invented his own prosthetic because he couldn't find one that allowed for the range of motion he needed to race again successfully. Called the Moto Knee and Versa Foot, his system utilizes a unique design that combines rugged, but lightweight materials with shock absorbers and spring actions to withstand participation in extreme sports. In less than two years after his accident, Schultz won both the silver and gold medals in the Adaptive Motocross games and started BioDapt to produce these prosthetics for other athletes to use in competition.

## Upper-Limb Prosthetics

Though lower-limb prosthetics get a great deal of press due to their extraordinary design and performance, upper-limb sports prosthetics for athletes also combine advanced technology with hybrid materials so that athletes can experience their chosen sport. Specially-modified prosthetics like the Viau system for swimming, the Eagle for golfing, the Pinch Hitter for baseball, the Power Play for hockey, or hooks for bicycling all work to mimic the functions of fingers, arms, and elbows.



**AGH**

AKADEMIA GÓRNICZO-HUTNICZA  
IM. STANISŁAWA STASZICA  
W KRAKOWIE

**"You'll never be able to replace the limb, but we can get things like ground reaction force, the spring in the feet, things like that. And now we have athletes who are using these devices to beat world records."**

John Spillar, market manager for sports prosthetics for Ottobock



When the IAAF ( International Association of Athletics Federations ) weighed in on Pistorius and his flex-foot Cheetah blades, they cited their own study, which found, "The positive work, or returned energy, from the prosthetic blade is close to three times higher, than with the human ankle joint in maximum sprinting." A durable, powered prosthetic leg with a smart microprocessor, custom engineered to play basketball, might have the same kind of advantage over the weary limbs of guys playing 2,500 minutes a season ( NBA contract ).

"The technology in the last five years is leaps and bounds ahead of where it was the previous 15 years," says John Spillar, market manager for sports prosthetics in North America for Ottobock, a manufacturer of prosthetics. "We're making more and more custom devices for people who want to climb mountains, for people who want to play specific sports. You'll never be able to replace the limb, but we can get things like ground reaction force, the spring in the feet, things like that, and now we have athletes who are using these devices to beat world records."

"Sports and the military have driven most of the technical advances in lower limb prosthetic devices," says Cooper, a veteran who suffered a spinal cord injury. "Both have pushed technology to achieve higher levels of performance, one for sports and one for tactical movement. Energy-storing feet, carbon fiber sockets, shock-absorbing pylons are all examples of advances from striving to improve performance in sports and military activities."

Some might question whether the player's production is truly his own creation. As Huber says, "Are you observing the talent of a human, or are you observing the talent of a software engineer?" Sports is where people go to test the physical potential of the human body, and there will be those who believe that a creation like a robotic prosthetic introduces an inhuman element to a fundamentally human endeavor. For people nervous about the prospect of artificial intelligence colonizing the human race, this might seem like the gateway technology to cyborgs. Mechanization has a prominent place in sports, whether the advent is compression sleeves, cryo chambers or platelet-rich plasma therapy. Laser eye surgery requires no permission, and professional athletes are on the frontier of medical advancement, whether they're traveling to Germany for surgery or tracking their exertion by running around the floor with a GPS device attached to their bodies. These innovations don't rouse fears primarily because they're available to every competitor. Enhancement, whether we're talking about a powered prosthetic or an athlete whose parents elected to have his blood's oxygen content increased while he was in the womb, will almost certainly land on sports' ethical agenda in the next few decades. It will also do something not seen since the advent of the Olympics, or the introduction of women teams, or the rise of advanced surgical procedures that would've been inconceivable a generation ago: It will test the world's definition of "athlete."

The purpose  
of prosthetics  
is not always  
to replace , but  
sometimes to  
**ENHANCE**  
HUMAN OR ANIMAL'S BIOMECHANICAL  
CAPABILITIES



THAT PART OF THE PROJECT FOCUSES ON  
THE WORK DONE SO FAR TO UNDERSTAND  
THE EVOLUTION AND MORPHOLOGY OF  
THE HUMAN THUMB AND HOW ITS  
SPECIAL BIOMECHANICAL FEATURES  
ARE EFFICIENTLY USED IN

## ANTHROPOMORPHIC ROBOTIC HAND DESIGNS

Human hand is a complex biomechanical structure with interconnected bones, joints, muscles, tendons, ligaments, nerves, and numerous sensors. Hand's dexterity is attributed to its around 20 number of Degrees of Freedom (DOFs) (ElKoura and Singh). However mine is designed to have 27 DOFs: 5 for each finger and all of them attached to the wrist with 2 DOF connection (I wanted to use the roller with 3 DOFs, however I noticed that the rotation comes from the elbow, not from the joint connecting radius and ulna with the wrist bones). Among the five digits in the hand, the thumb is the most independent (Ingram et al., 2008) and is also different in terms of kinematics, size, and strength of its muscles. Therefore, this review focuses on human biomechanics of the thumb together with work done on robotic counterparts. Evolution of primate hand is greatly related to its interaction with the environment in food prehension strategies, available resources, and tool making (Kivell, 2015). Early human ancestors started exploring the environment using their hands once they developed bipedal locomotion 15 million years ago (Flatt, 2002). Evidence found in fossil hominins indicates that hand's unique capabilities co-evolved with its morphology (Marzke, 2013). Early tool use studies indicate that human thumb's adaptation to create forceful precision grips and ability to resist large forces in using earliest stone tools (Oldowan) is due to relatively long thumb with shorter fingers and complex intrinsic/extrinsic muscle structure (Rolian et al., 2011). Authors in Almécija et al. (2015) compare thumb-to-finger ratio among modern apes and modern humans (Figure 1).

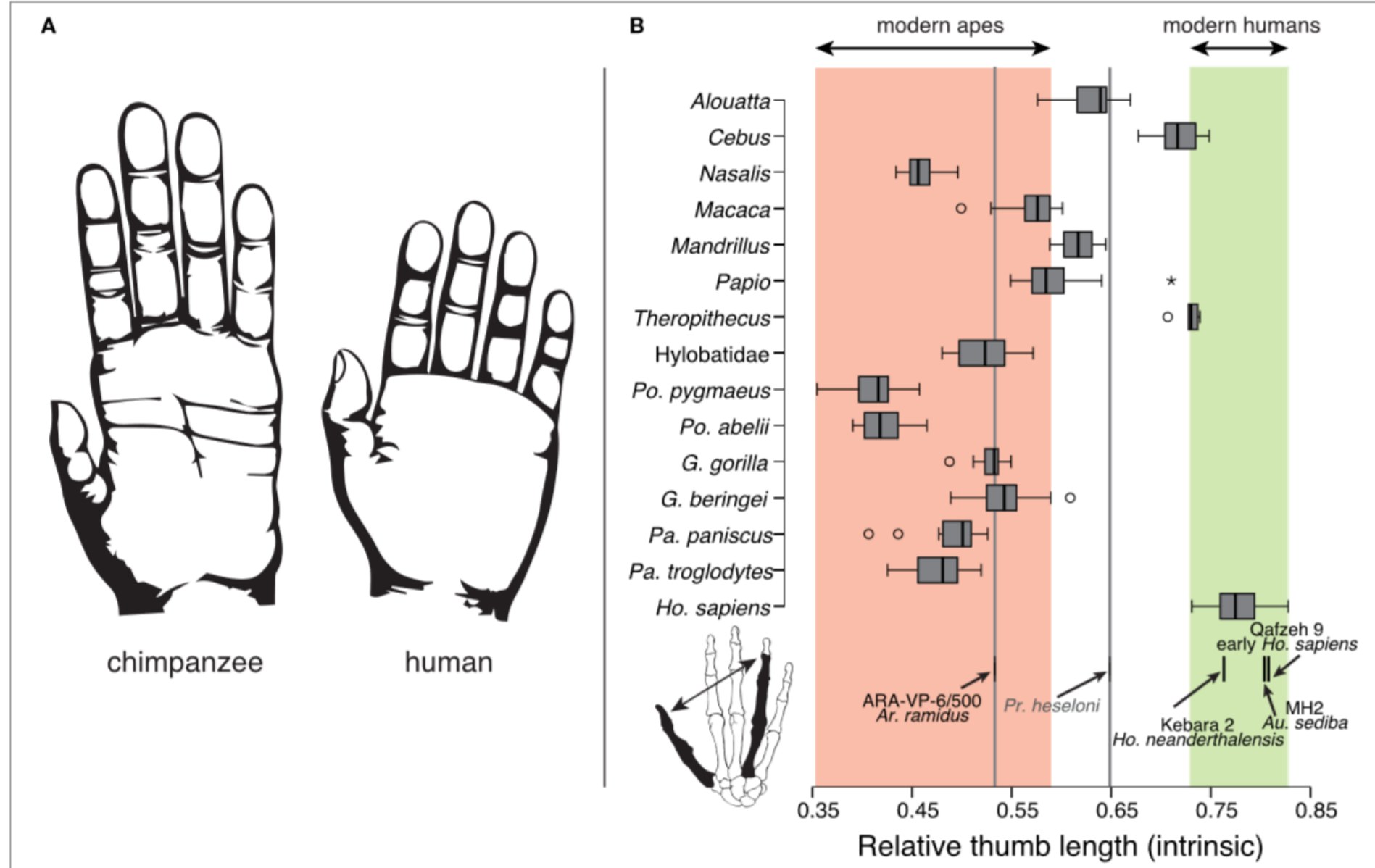


**FIGURE 1 | (A)** Chimpanzee and human hand comparison. **(B)** Thumb-to-fourth finger length ratios of modern apes and modern humans. Corresponding ranges are highlighted in red and green, respectively. The figure is reprinted with kind permission from Almécija et al. (2015).

Their analysis shows that high thumb-to-finger ratio in humans did not change since the last common ancestors of humans and chimpanzees. The hand anatomy evolved inclusively in the palm and the thumb due to its adaptation in grasping spheroids and cylinders (Young, 2003). Hence these grasps are defined as throwing grips and clubbing grips. It has been argued that the evolution of the precision grasp in addition to the power grasp enabled human to perform in-hand manipulation of objects (Pouydebat et al., 2008). Napier (1956) classifies most grasp types into the following two different groups: power grasp and precision grasp. In power grasp, the object is held between palm and the finger surfaces with primary need for force. In precision grasp, the object is held with the tips of the fingers and the thumb with less force and high precision.



THAT PART OF THE PROJECT FOCUSES ON  
THE WORK DONE SO FAR TO UNDERSTAND  
THE EVOLUTION AND MORPHOLOGY OF  
THE HUMAN THUMB AND HOW ITS  
SPECIAL BIOMECHANICAL FEATURES  
ARE EFFICIENTLY USED IN

## ANTHROPOMORPHIC ROBOTIC HAND DESIGNS

Grasps are further subdivided into grasp taxonomies according to the object geometry and associated hand configurations (Cutkosky and Howe, 1990; Feix et al., 2009). In grasping objects, fingers, palm, and the thumb share forces jointly. Three such distinctive force-sharing pairs are identified as follows: (1) pad, between the pads of the fingers and the thumb, (2) palm, between the fingers and the palm, and (3) side, between the thumb and the side of the index finger (Cutkosky and Howe, 1990).

Recently, existing human grasp taxonomies are analyzed and integrated into a new taxonomy called "The Grasp Taxonomy" (Feix et al., 2016). Thumb's key role in grasping objects is highlighted in this taxonomy by rearranging grasps according to thumb's Adduction-Abduction (A-A) motion. Human thumb along with the foldable palm contributes to make oblique arches that help to stabilize orientations and positions of the fingers in in-hand manipulation of objects (Sangole and Levin, 2008). Early stages of robotic end effectors performed highly dexterous tasks without mimicking the human hand, for example, SARAH hand (Rubinger et al., 2001), AMADEUS hand (Lane et al., 1999). Some designs even adopt predatory bird-grasping behavior (Ramos et al., 1999). It is often argued that anthropomorphism is not a necessity in robotic hand dexterity unless the robotic hand is used in prosthesis, rehabilitation, or human-oriented purposes (Gama Melo et al., 2014).

Anthropomorphic geometry is introduced with thumb kinematics different from those of fingers in the Utah/MIT hand (Jacobsen et al., 1986) (Figure 2A). However, there are some simplifications due to practical limitations. From then onward, many robotic hands have been developed (Parida, 2013), mimicking human hand functionality (Martell and Gini, 2007). Due to their innate complex actuation strategies and cost, they are not good choices for prosthesis or wearable hands. In contrast, passively adaptive and underactuated hands are simpler in design and better for grasping in unstructured environments yet proved less dexterous (Ciocarlie and Allen, 2010).

The present prosthetic hands are not dexterous enough mainly due to the lack of functional thumbs (Carrozza et al., 2006). Adequate placement of the thumb at the right moment determines whether a grasp is successful or not (Cotugno et al., 2014). It is important to abstract the functionality of the human thumb rather than creating a mechanical copy of its biology (Chalon et al., 2010). Thumbs in robotic hands (Gebenstein, 2012) and in exoskeletons (Heo et al., 2012) are designed based on various kinematic models.

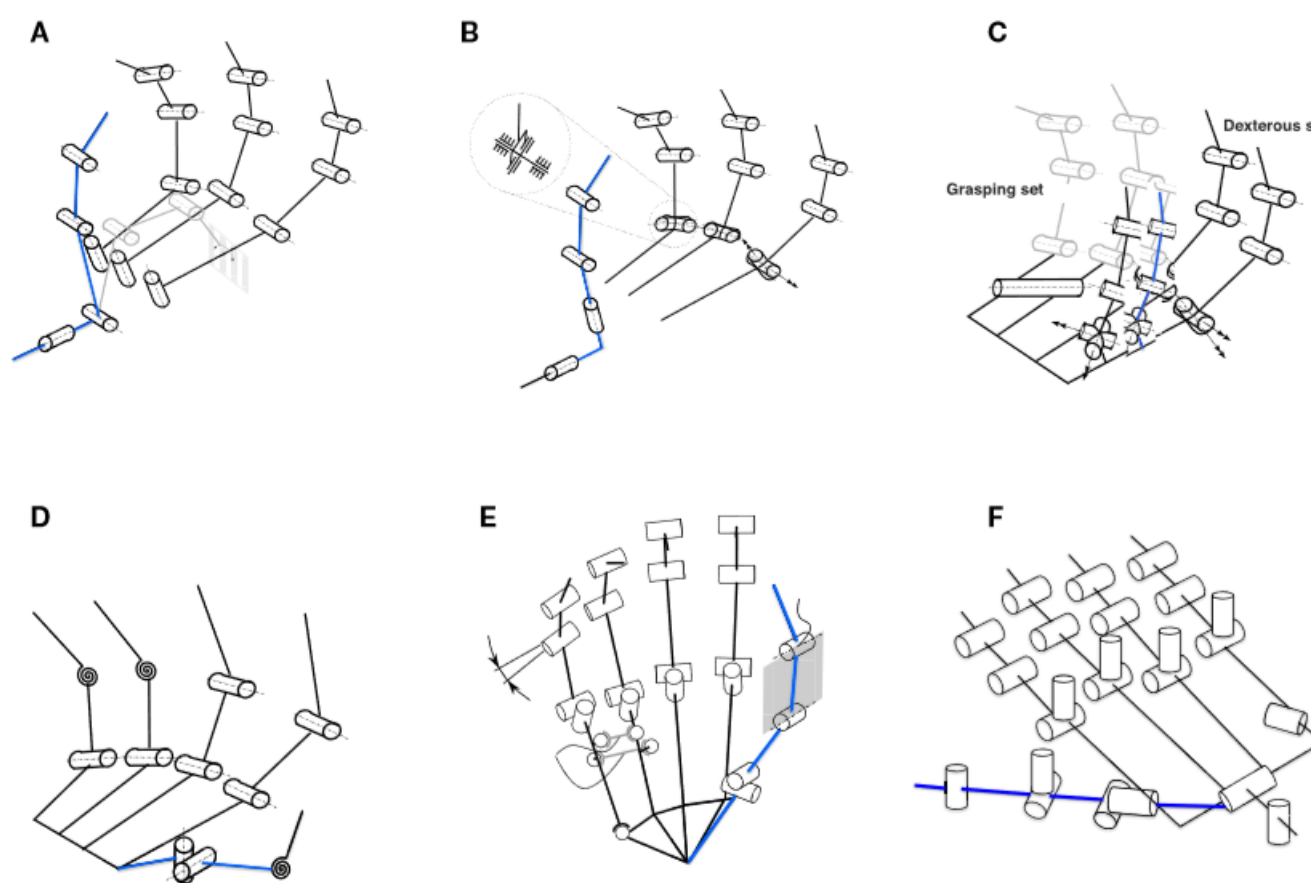


**FIGURE 2** | Biomimetic thumb designs (highlighted in blue) in some selected robotic hands. The kinematic models are reprinted and highlighted with kind permission from Gebenstein (Gebenstein, 2012) and Walker (Greenhill et al., 2010). **(A)** Utah/MIT hand (Jacobsen et al., 1986)—two thumb proximal joint axes are separated and thumb base is placed on the palm between first and second fingers with its proximal axis parallel to the palm plane to reduce tendon routing complexity. **(B)** Twenty-one hand (Iwata and Sugano, 2009)—similar to the Utah/MIT hand, the two thumb proximal joint axes are separated. However, the second axis is designed to avoid thumb singularity. **(C)** Robonaut hand (Lovichik and Diftler, 1999)—thumb has same finger kinematic structure and is not positioned directly opposed to the fingers. Thumb base yaw is 70° and pitch is 110° to increase its ROM. **(D)** ARMAR hand (Fukaya et al., 2000)—thumb has only 1-DOF with its rotational axis set at an angle of 6.5° to the vertical line. AA axis is positioned proximal to the palm to avoid singularity. **(E)** Awiwi hand (Gebenstein, 2012)—thumb has four DOFs to agree with the DLR hand arm system. Inclinations are introduced in the IP and MCP joints to improve opposition and power grasp. Thumb TM joint axes are orthogonal but not intersecting. **(F)** Shadow hand (Greenhill et al., 2010)—24-DOF shadow hand has a five-DOF thumb fully actuated using air muscles or smart motors. Thumb is positioned on the front of the palm with its A-A axis inclined with respect to the index finger (Gebenstein, 2012).

THAT PART OF THE PROJECT FOCUSES ON  
THE WORK DONE SO FAR TO UNDERSTAND  
THE EVOLUTION AND MORPHOLOGY OF  
THE HUMAN THUMB AND HOW ITS  
SPECIAL BIOMECHANICAL FEATURES  
ARE EFFICIENTLY USED IN

## ANTHROPOMORPHIC ROBOTIC HAND DESIGNS

When any hand function is performed (grasp or manipulation), the real axis movement occurs not along the exact joint axes of the thumb (Griffin et al., 2000). Based on the anatomical context, the overall musculoskeletal structure plays a pivotal role in natural human thumb movement (Figures 3 and 4). In addition to the muscle structure, there are other supportive mechanisms including ligaments and tendons that help to maintain stability in various proportions depending on the thumb's position and forces it encounters in functional activities.

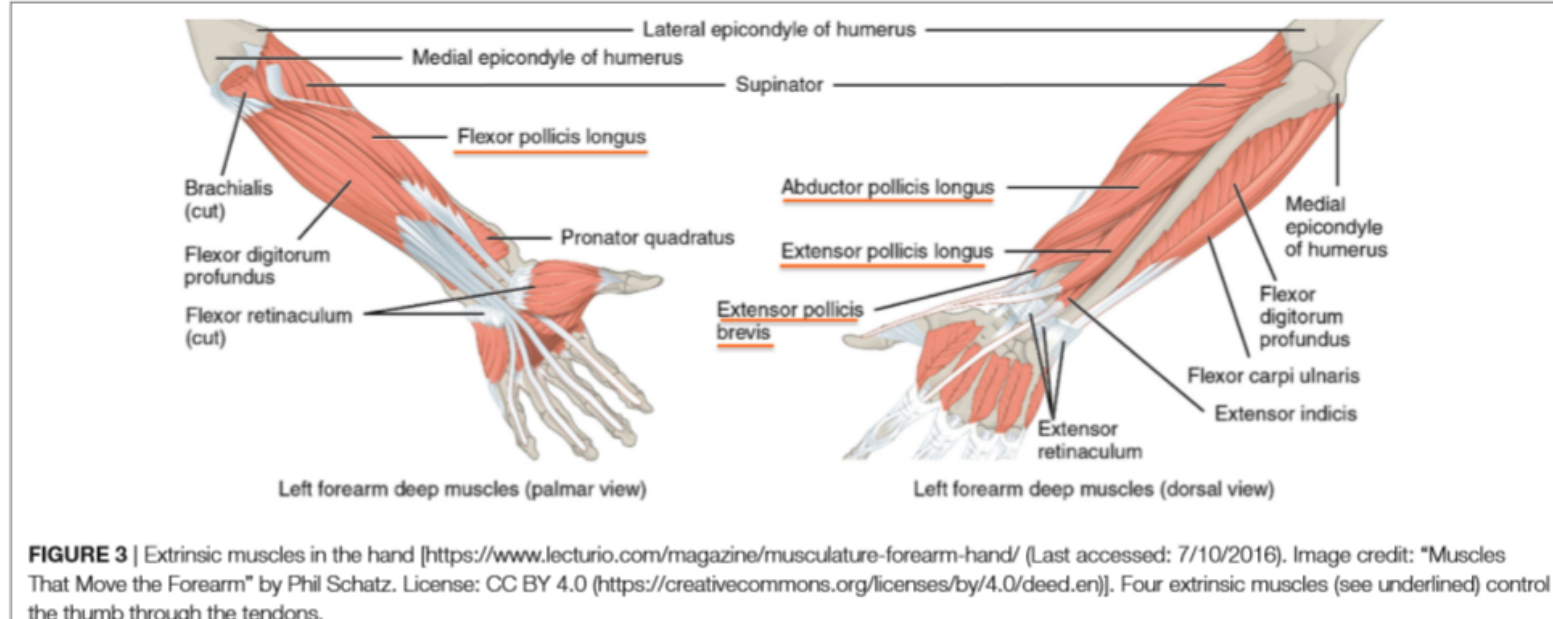


**FIGURE 3** | Extrinsic muscles in the hand [<https://www.lecturio.com/magazine/musculature-forearm-hand/>] (Last accessed: 7/10/2016). Image credit: "Muscles That Move the Forearm" by Phil Schatz. License: CC BY 4.0 (<https://creativecommons.org/licenses/by/4.0/deed.en>). Four extrinsic muscles (see underlined) control the thumb through the tendons.

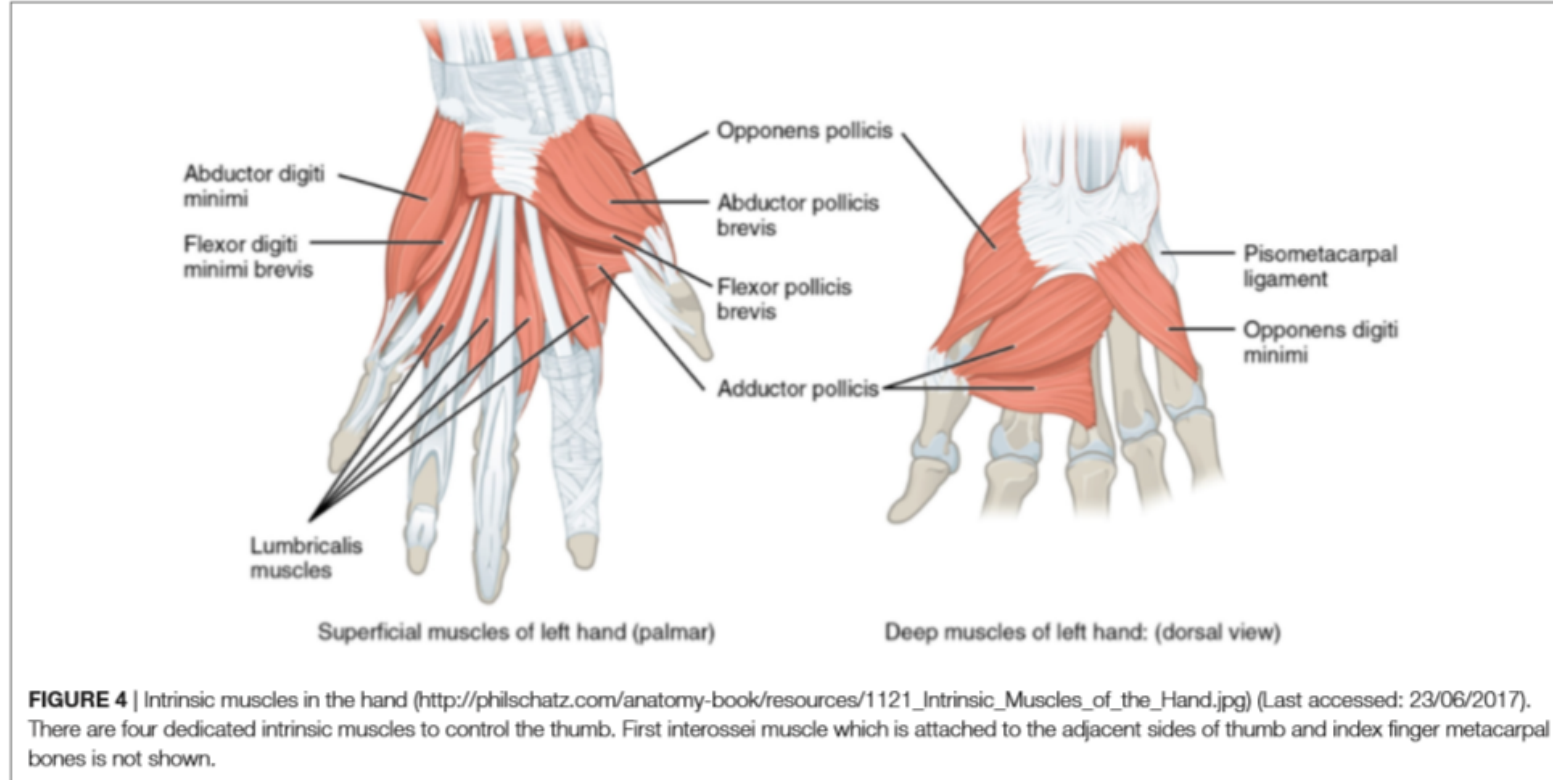


**FIGURE 4** | Intrinsic muscles in the hand ([http://philschatz.com/anatomy-book/resources/1121\\_Intrinsic\\_Muscles\\_of\\_the\\_Hand.jpg](http://philschatz.com/anatomy-book/resources/1121_Intrinsic_Muscles_of_the_Hand.jpg)) (Last accessed: 23/06/2017). There are four dedicated intrinsic muscles to control the thumb. First interossei muscle which is attached to the adjacent sides of thumb and index finger metacarpal bones is not shown.

The anatomy of the hand is extremely complex, intricate, and fascinating, probably the most complex of all the joints in the body. There are several important tendons that cross the wrist. Tendons connect muscles to bone. The tendons that cross the wrist begin as muscles that start in the forearm. Those that cross the palm side of the wrist are the flexor tendons. They curl the fingers and thumb, and they bend the wrist. The flexor tendons run beneath the transverse carpal ligament. This structure lies on the palm side of the wrist. This band of tissue keeps the flexor tendons from bowing outward when you curl your fingers, thumb, or wrist. The tendons that travel over the back of the wrist, the extensor tendons, run through a series of tunnels, called compartments. These compartments are lined with a slick substance called tenosynovium, which prevents friction as the extensor tendons glide inside their compartment. Its integrity is absolutely essential for our everyday functional living. Our fingers are controlled by the tendons attached to the muscles of the hand. Our neural system takes care about every aspect of motion in our body. Therefore, it is possible to make a prosthetic hand, that can be controlled by the human through the EEG or EMG signals.



THAT PART OF THE PROJECT FOCUSES ON THE WORK DONE SO FAR TO UNDERSTAND THE EVOLUTION AND MORPHOLOGY OF THE HUMAN THUMB AND HOW ITS SPECIAL BIOMECHANICAL FEATURES ARE EFFICIENTLY USED IN

## ANTHROPOMORPHIC ROBOTIC HAND DESIGNS

There are four main groups of intrinsic muscles in the hand: thenar muscles move the thumb, hypothenar muscles move the little finger, the interosseous muscles, and the lumbricals move the other fingers. Each finger has a proximal, middle, and distal phalanx (phalanges), whereas the thumb has only a proximal and distal phalanx (Figure 5). Metacarpal bones comprise the palm. Wrist is made up from carpal bones. The joints between the carpal and metacarpal bones are called carpometacarpals. MetaCarpoPhalangeal (MCP) joints are between the metacarpals and proximal phalanges. Proximal InterPhalangeal (IP) and distal IP joints are between phalanges, whereas thumb has only one IP joint. Human thumb has three joints: TM, MCP, and IP (since the first metacarpal of the thumb and the trapezium form the CarpoMetaCarpal (CMC) joint, it is termed separately as TM). Within the thumb, TM joint's unique saddle shape along with its unique muscle and ligament capsule contributes significantly to the stability and dexterity of any grasp (Neumann and Bielefeld, 2003). Moreover, thumb's contribution in the following three unique manipulative abilities of the human hand are identified (Kivell, 2015): the ability to rotate and in-hand manipulate objects between the thumb and the fingertips, the ability to forcefully stabilize or manipulate the grasped object between the thumb pad and one or more fingers, and the forceful grasp of cylindrical objects with the thumb either wrapping around like in a fist or stretched. It is evaluated that the loss of the thumb corresponds to a loss of 40% of the hand functions (Hart et al., 1993). The thumb is the only digit of the hand, which can be opposed to the other four fingers, although it is composed of only two bones: the proximal and distal phalanxes. The opposition mechanism, however, involves a larger set of bones (Figure 5), namely the trapezium, the trapezoid, and the scaphoid (Kapandji, 1982). Yet there is no common agreement on how the mechanism works in detail (Emerson et al., 1996). The thumb is the only finger whose IP joint can be bent backward when the digit is fully abducted from the palm (hitchhiker's thumb) (Gray, 1918).

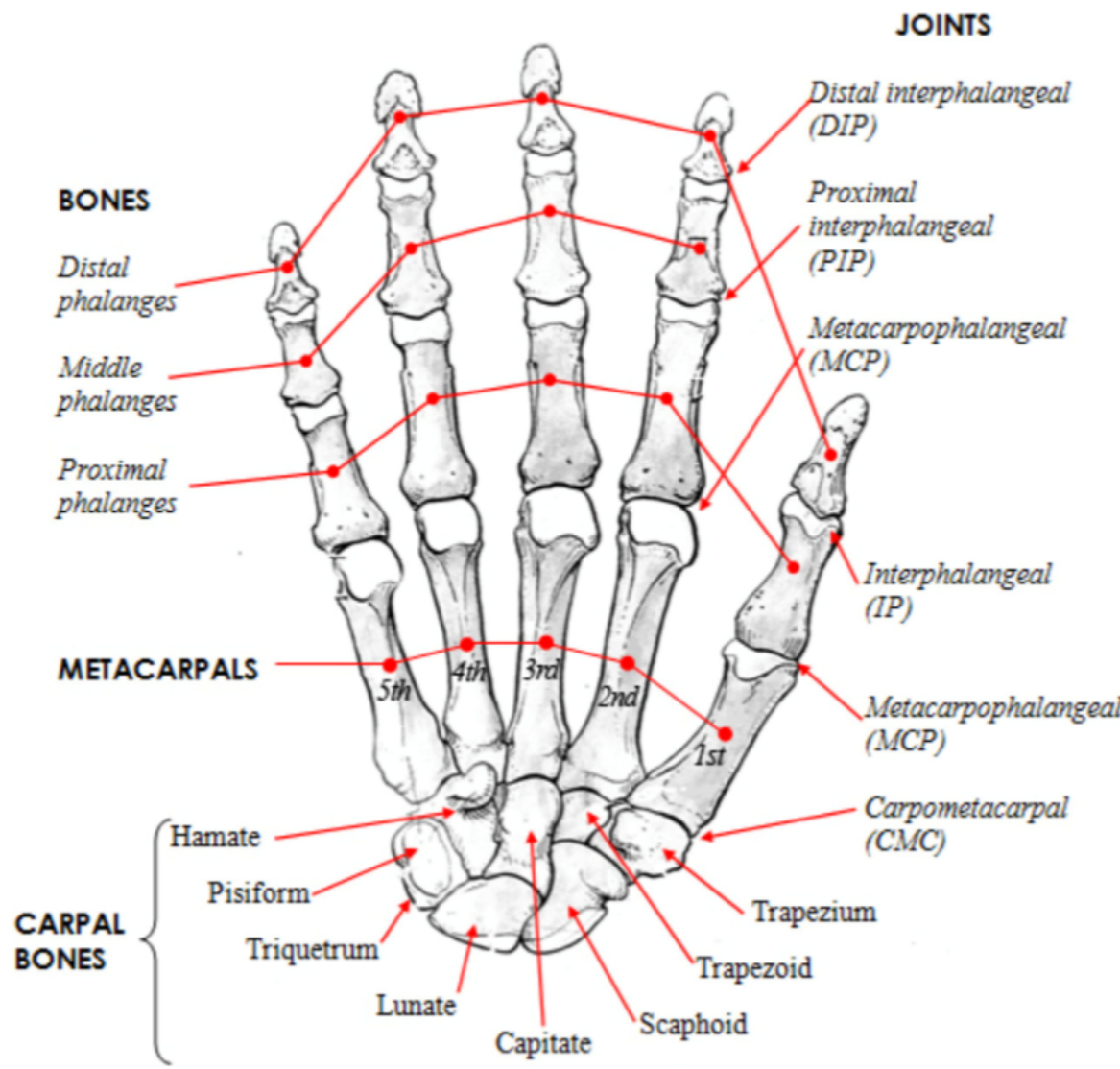
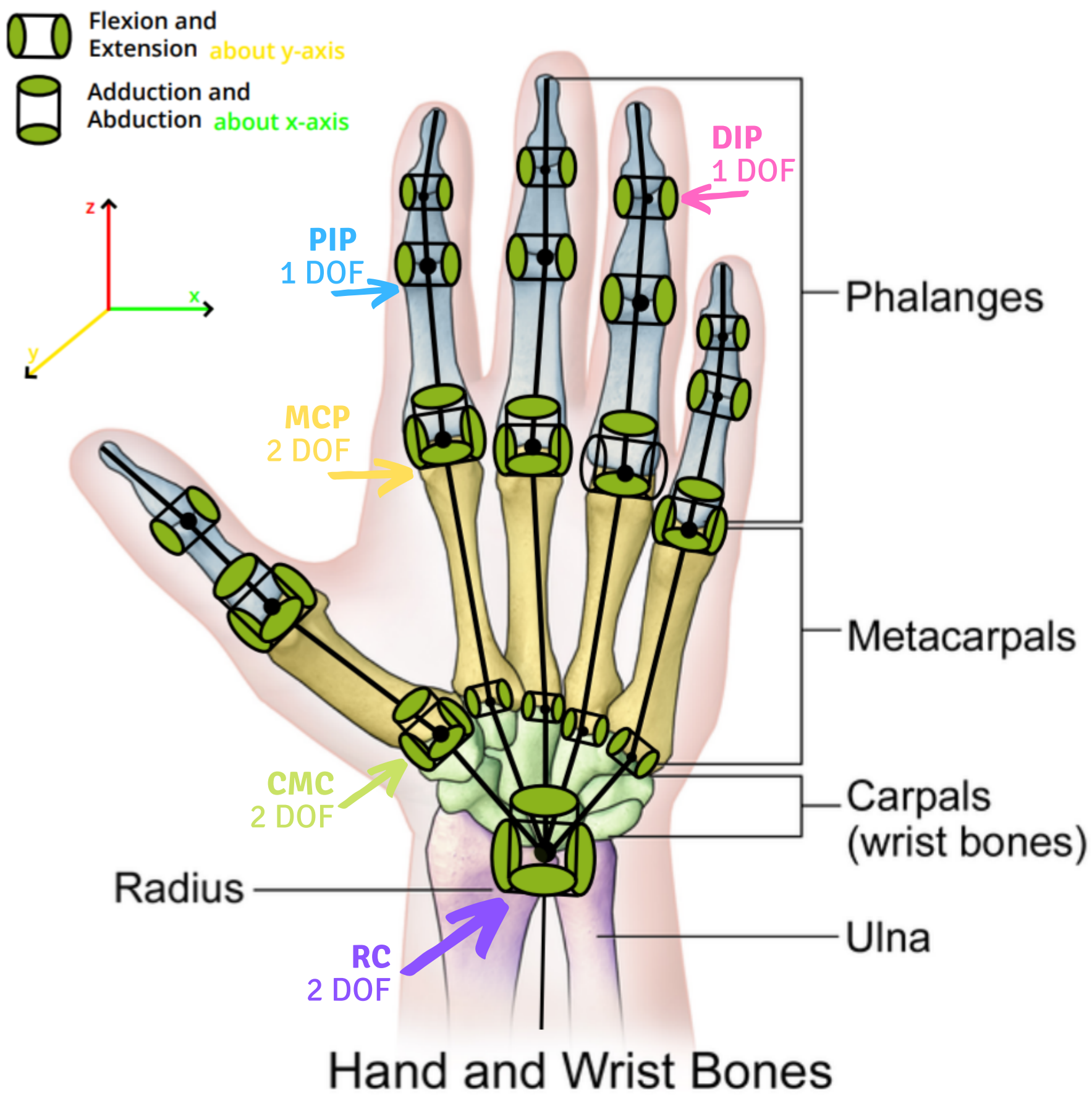


FIGURE 5 | Human hand skeletal structure depicting finger bones, joints, metacarpals, and carpal bones [<http://www.amulyabharat.com/hand-bone-anatomy-human-diagram-download/> (Last accessed: 7/10/2016)].

For these reasons, the kinematic model of the thumb is one of the main sources of variability in designing kinematics of human hands, as kinematic models may vary between 15 (Bianchi et al., 2013) and 25 DOFs (Santello et al., 2013).

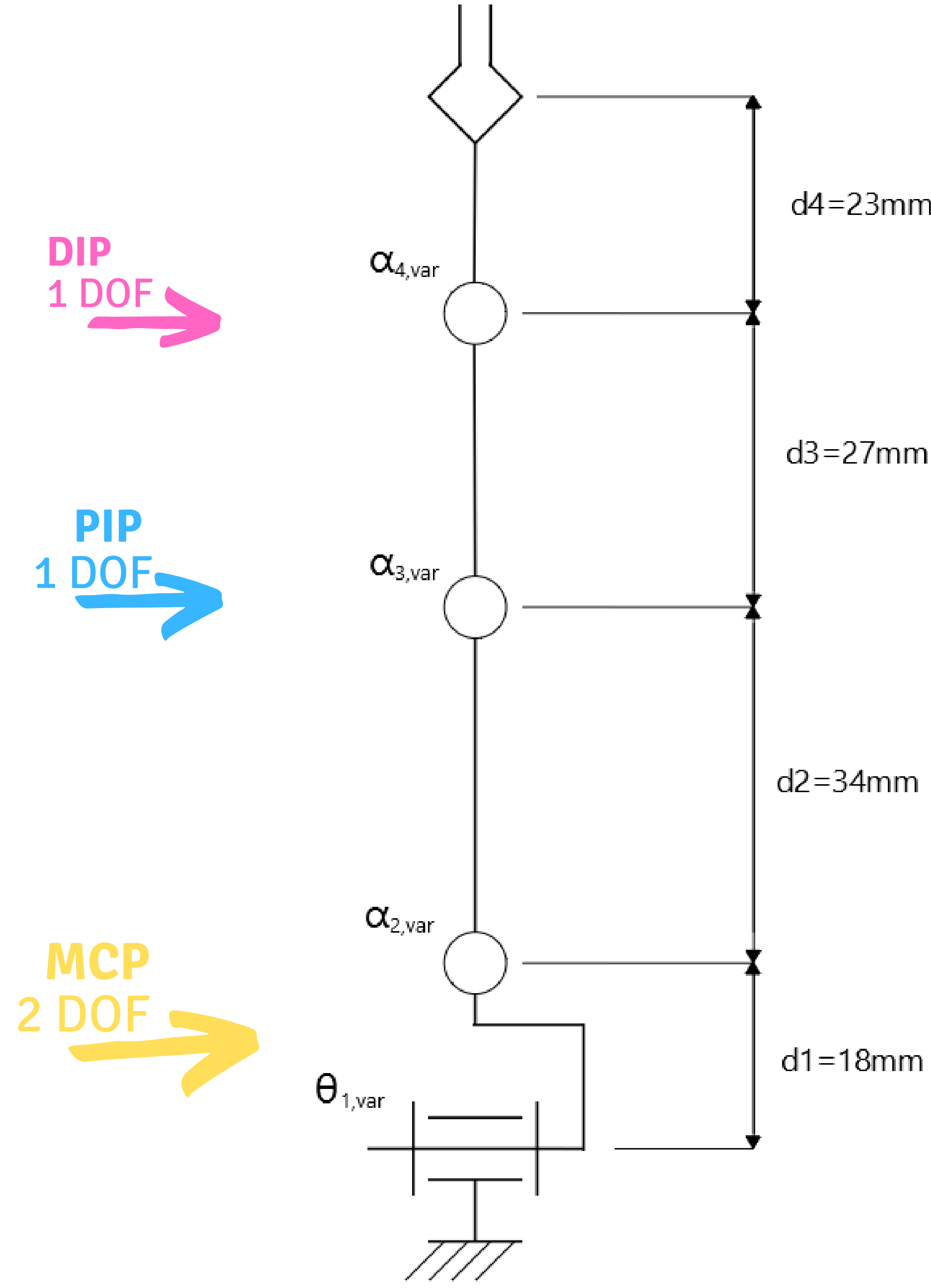
TOP VIEW ON MY HUMAN HAND KINEMATIC SCHEME  
DESIGN

The hand joints are classified into three main types: hinge (1 DoF), condyloid (2 DoFs) and saddle (2 DoFs) joints. The hinge joints on the human hand are the CMC, PIP and the DIP joints. They allow the fingers to flex (move toward the palm) and to extend (move further from palm). The condyloid joints are the finger MCP joints that allow flexion/extension and abduction/adduction of the fingers, the latter being the motion of spreading and gathering them. Hence, each finger can be represented as a kinematic serial chain of 5 DoFs: 1 at the CMC, 2 at the MCP, 1 at the PIP and a last one at the DIP. Finger PIP and DIP joints are orthogonal to the bone axis when the phalanx is fully extended and they progressively bend toward the middle (due to the bone surface) while flexing. As a result, all fingers converge to a common point improving the opposition of the thumb to the ring and little fingers. According to Vitruvian man's hand and the study conducted by Isobe, human fingertips approximatively lie on a common circle when abducted. The circle has a radius equal to the middle finger length and it is centered at the MCP joint of the middle finger. The thumb has the same number of DoFs of fingers but differently distributed: the RC joint is a saddle joint (connection between thumb, fingers and wrist bones with the radius and ulna bones), the MCP is a condyloid joint and the IP joint is a hinge joint. The thumb is the only finger able to turn and oppose to the other four fingers. The opposability of the thumb enables humans to grip and hold objects that they would not be able to take otherwise. Not all DoFs in the human hand are independent. Tendons couple some joints like the PIP and DIP joints of the fingers.

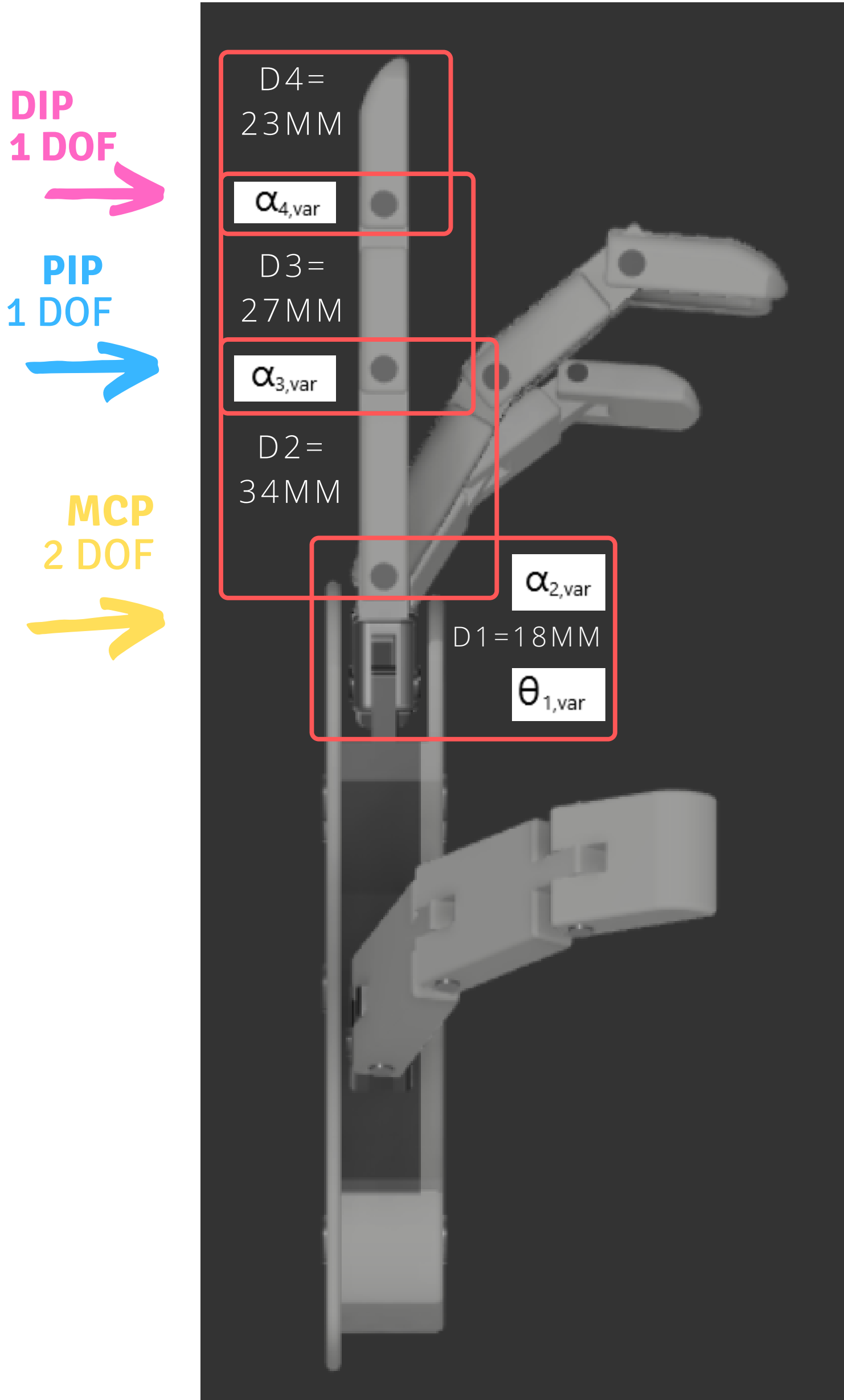
## SIDE VIEW OF MY HUMAN SECOND FINGER KINEMATIC SCHEME AFTER SIMPLIFICATION

INSTEAD OF A 5DOF FINGER AND 27DOF HUMAN HAND MODEL , MR. TOMASZ BURATOWSKI PHD. ENG. HAS HELPED ME TO COME UP WITH THE IDEA FOR NEW , SIMPLIFIED VERSION OF A 4DOF FINGER AND 20DOF HUMAN HAND PROSTHESIS MODEL.

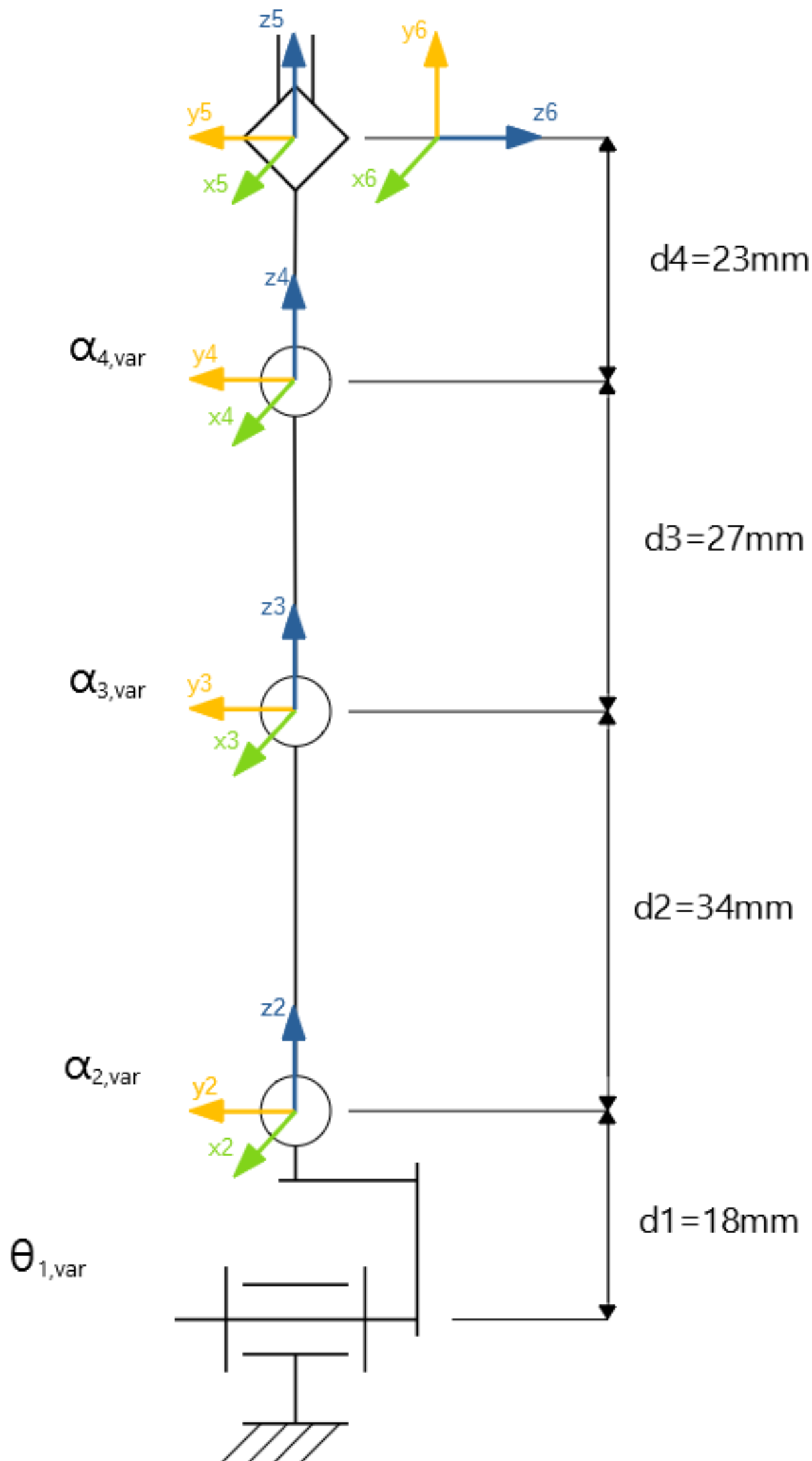
THE SIMPLIFICATION OCCURED DUE TO VERY SMALL RANGES OF MOTION IN THE CMC AND RC JOINTS , WHICH I WAS ABLE TO NEGLECT IN THE KINEMATICS CALCULATIONS AND THEN IN FINAL MODEL.



## SIDE VIEW OF THE SIMPLIFIED SECOND FINGER MODEL



# SOLUTION ATTEMPT USING DENAVIT-HARTENBERG NOTATION



THE TABLE BELOW SHOWS KINEMATIC PARAMETERS ,WHICH ARE BASED ON THE KINEMATIC CHAIN WITH THREE DIMENSIONAL COORDINATE SYSTEMS CONNECTED TO EACH JOINT.

	$\theta_i$	$d_i$	$a_i$	$\alpha_i$
1	$\theta_{1var}$	0	0	+90°
2	0	$d_1$	0	$\alpha_{2var}$
3	0	$d_2$	0	$\alpha_{3var}$
4	0	$d_3$	0	$\alpha_{4var}$
5	0	$d_4$	0	-90°



BASING ON THE TABLE LOCATED ON THE PREVIOUS PAGE I CREATED HOMOGENEOUS TRANSFORMATION MATRICES FOR EACH OF THE LINK IN THE KINEMATIC CHAIN. THESE EQUATIONS WILL BE NEEDED FOR OBTAINING THE FORWARD KINEMATICS OF MY SECOND FINGER PROSTHESIS.

$$A_1 = \text{Rot}_{z,\theta_{1var}} \cdot \text{Rot}_{x,90^\circ}$$

$$A_1 = \begin{bmatrix} \cos(\theta_{1var}) & -\sin(\theta_{1var}) & 0 & 0 \\ \sin(\theta_{1var}) & \cos(\theta_{1var}) & 0 & 0 \\ 0 & 0 & 1 & 0 \\ 0 & 0 & 0 & 1 \end{bmatrix} \cdot \begin{bmatrix} 1 & 0 & 0 & 0 \\ 0 & \cos(90^\circ) & -\sin(90^\circ) & 0 \\ 0 & \sin(90^\circ) & \cos(90^\circ) & 0 \\ 0 & 0 & 0 & 1 \end{bmatrix} = \begin{bmatrix} \cos(\theta_{1var}) & 0 & \sin(\theta_{1var}) & 0 \\ \sin(\theta_{1var}) & 0 & -\cos(\theta_{1var}) & 0 \\ 0 & 1 & 0 & 0 \\ 0 & 0 & 0 & 1 \end{bmatrix}$$

$$A_2 = \text{Trans}_{z,d_1} \cdot \text{Rot}_{x,\alpha_{2var}}$$

$$A_2 = \begin{bmatrix} 1 & 0 & 0 & 0 \\ 0 & 1 & 0 & 0 \\ 0 & 0 & 1 & d_1 \\ 0 & 0 & 0 & 1 \end{bmatrix} \cdot \begin{bmatrix} 1 & 0 & 0 & 0 \\ 0 & \cos(\alpha_{2var}) & -\sin(\alpha_{2var}) & 0 \\ 0 & \sin(\alpha_{2var}) & \cos(\alpha_{2var}) & 0 \\ 0 & 0 & 0 & 1 \end{bmatrix} = \begin{bmatrix} 1 & 0 & 0 & 0 \\ 0 & \cos(\alpha_{2var}) & -\sin(\alpha_{2var}) & 0 \\ 0 & \sin(\alpha_{2var}) & \cos(\alpha_{2var}) & d_1 \\ 0 & 0 & 0 & 1 \end{bmatrix}$$

$$A_3 = \text{Trans}_{z,d_2} \cdot \text{Rot}_{x,\alpha_{3var}}$$

$$A_3 = \begin{bmatrix} 1 & 0 & 0 & 0 \\ 0 & 1 & 0 & 0 \\ 0 & 0 & 1 & d_2 \\ 0 & 0 & 0 & 1 \end{bmatrix} \cdot \begin{bmatrix} 1 & 0 & 0 & 0 \\ 0 & \cos(\alpha_{3var}) & -\sin(\alpha_{3var}) & 0 \\ 0 & \sin(\alpha_{3var}) & \cos(\alpha_{3var}) & 0 \\ 0 & 0 & 0 & 1 \end{bmatrix} = \begin{bmatrix} 1 & 0 & 0 & 0 \\ 0 & \cos(\alpha_{3var}) & -\sin(\alpha_{3var}) & 0 \\ 0 & \sin(\alpha_{3var}) & \cos(\alpha_{3var}) & d_2 \\ 0 & 0 & 0 & 1 \end{bmatrix}$$

$$A_4 = \text{Trans}_{z,d_3} \cdot \text{Rot}_{x,\alpha_{4var}}$$

$$A_4 = \begin{bmatrix} 1 & 0 & 0 & 0 \\ 0 & 1 & 0 & 0 \\ 0 & 0 & 1 & d_3 \\ 0 & 0 & 0 & 1 \end{bmatrix} \cdot \begin{bmatrix} 1 & 0 & 0 & 0 \\ 0 & \cos(\alpha_{4var}) & -\sin(\alpha_{4var}) & 0 \\ 0 & \sin(\alpha_{4var}) & \cos(\alpha_{4var}) & 0 \\ 0 & 0 & 0 & 1 \end{bmatrix} = \begin{bmatrix} 1 & 0 & 0 & 0 \\ 0 & \cos(\alpha_{4var}) & -\sin(\alpha_{4var}) & 0 \\ 0 & \sin(\alpha_{4var}) & \cos(\alpha_{4var}) & d_3 \\ 0 & 0 & 0 & 1 \end{bmatrix}$$

$$A_5 = \text{Trans}_{z,d_4} \cdot \text{Rot}_{x,-90^\circ}$$

$$A_5 = \begin{bmatrix} 1 & 0 & 0 & 0 \\ 0 & 1 & 0 & 0 \\ 0 & 0 & 1 & d_4 \\ 0 & 0 & 0 & 1 \end{bmatrix} \cdot \begin{bmatrix} 1 & 0 & 0 & 0 \\ 0 & \cos(-90^\circ) & -\sin(-90^\circ) & 0 \\ 0 & \sin(-90^\circ) & \cos(-90^\circ) & 0 \\ 0 & 0 & 0 & 1 \end{bmatrix} = \begin{bmatrix} 1 & 0 & 0 & 0 \\ 0 & 0 & 1 & 0 \\ 0 & -1 & 0 & d_4 \\ 0 & 0 & 0 & 1 \end{bmatrix}$$

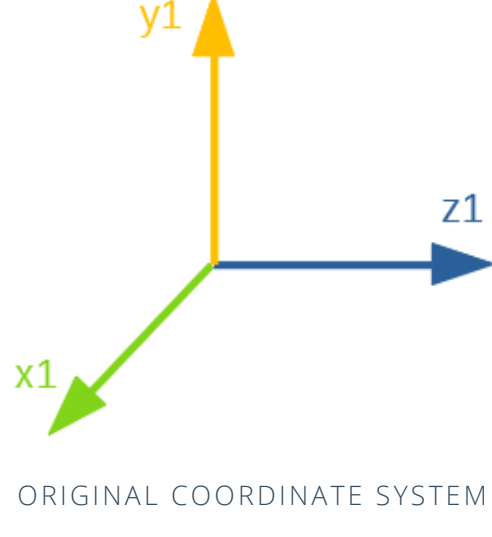
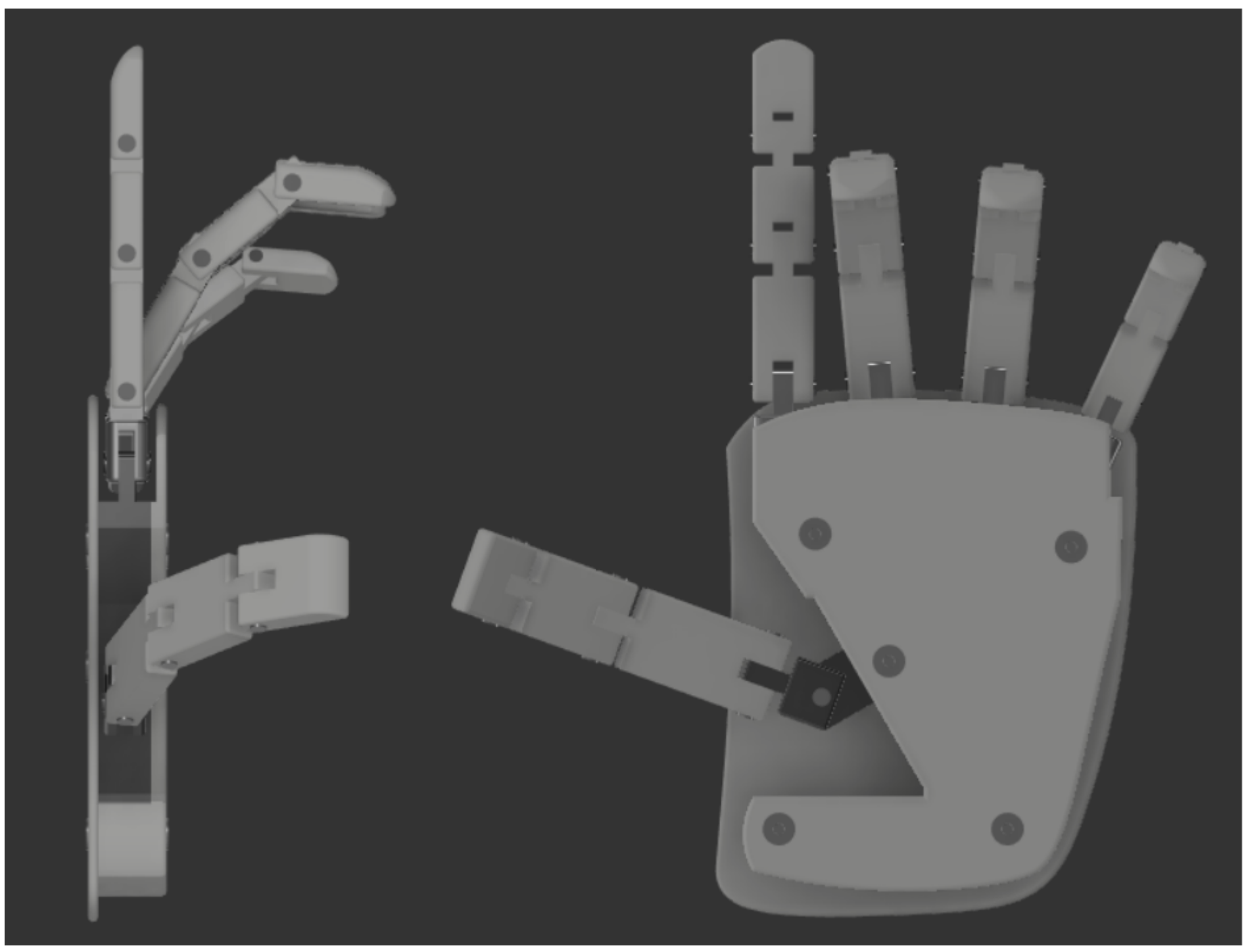
SUBSTITUTION TABLE :	
a = $\alpha_{2var}$	= $0^\circ$
b = $\alpha_{3var}$	= $0^\circ$
c = $\alpha_{4var}$	= $0^\circ$
d = $d_1$	= 18 mm
e = $d_2$	= 34 mm
f = $d_3$	= 27 mm
g = $d_4$	= 23 mm
k = $\theta_{1var}$	= $0^\circ$

THE FINAL TRANSFORMATION MATRIX IS OBTAINED BY MULTIPLICATION OF THE HOMOGENOUS TRANSFORMATION MATRICES CORRESPONDING TO EACH JOINT.

$$T_{6,0} = A_1 \cdot A_2 \cdot A_3 \cdot A_4 \cdot A_5 =$$

$$\left( \begin{array}{ccc|c} \cos(k) & \frac{-\sin(a+b+c+k) + \sin(a+b+c-k)}{2} & \frac{-\cos(a+b+c+k) + \cos(a+b+c-k)}{2} & \frac{2 \times d \times \sin(k) + e \times \sin(a+k) + f \times \sin(a+b+k) + g \times \sin(a+b+c+k) - e \times \sin(a-k) - f \times \sin(a+b-k) - g \times \sin(a+b+c-k)}{2} \\ \sin(k) & \frac{\cos(a+b+c+k) + \cos(a+b+c-k)}{2} & \frac{-\sin(a+b+c+k) - \sin(a+b+c-k)}{2} & \frac{-2 \times d \times \cos(k) - e \times \cos(a+k) - f \times \cos(a+b+k) - g \times \cos(a+b+c+k) - e \times \cos(a-k) - f \times \cos(a+b-k) - g \times \cos(a+b+c-k)}{2} \\ 0 & \sin(a+b+c) & \cos(a+b+c) & -e \times \sin(a) - f \times \sin(a+b) - g \times \sin(a+b+c) \\ 0 & 0 & 0 & 1 \end{array} \right)$$





ORIGINAL COORDINATE SYSTEM

$$\begin{aligned}
 a &= \alpha_{2\text{var}} = 0^\circ \\
 b &= \alpha_{3\text{var}} = 0^\circ \\
 c &= \alpha_{4\text{var}} = 0^\circ \\
 d &= d_1 = 18 \text{ mm} \\
 e &= d_2 = 34 \text{ mm} \\
 f &= d_3 = 27 \text{ mm} \\
 g &= d_4 = 23 \text{ mm} \\
 k &= \theta_{1\text{var}} = 0^\circ
 \end{aligned}$$

FIRST POSITION OF THE DISTAL PHALANG OF THE SECOND FINGER  
REPRESENTED IN THE 3D CARTESIAN SYSTEM RESPECTIVELY TO THE LOCATION OF  
THE ORIGINAL COORDINATE SYSTEM:

$$\begin{aligned}
 X &= 0 \text{ MM} \\
 Y &= 102 \text{ MM} \\
 Z &= 0
 \end{aligned}$$

OBTAINED BY ADDING ALL OF THE PHALANG'S LENGTHS.  
 $D+E+F+G = 102\text{MM}$



I CHECKED IF THE FINAL TRANSFORMATION MATRIX IS CALCULATED CORRECTLY BY CHECKING THE SOLUTION IN MATLAB. I USED THE FOLLOWING CODE:

```
T6 = [
COS(K) -0.5*SIN(A+B+C+K)+0.5*SIN(A+B+C-K) -0.5*COS(A+B+C+K)+0.5*COS(A+B+C-K)
D*SIN(K)+0.5*E*SIN(A+K)+0.5*F*SIN(A+B+K)+0.5*G*SIN(A+B+C+K)-0.5*E*SIN(A-K)
-0.5*F*SIN(A+B-K)-0.5*G*SIN(A+B+C-K);

SIN(K) 0.5*COS(A+B+C+K)+0.5*COS(A+B+C-K) -0.5*SIN(A+B+C+K)-0.5*SIN(A+B+C-K)
-D*COS(K)-0.5*E*COS(A+K)-0.5*F*COS(A+B+K)-0.5*G*COS(A+B+C+K)-0.5*E*COS(A-K)
-0.5*F*COS(A+B-K)-0.5*G*COS(A+B+C-K);

0 SIN(A+B+C) COS(A+B+C) -E*SIN(A)-F*SIN(A+B)-G*SIN(A+B+C);

0 0 0 1
]
```

**T6** =

$$\begin{bmatrix} 1 & 0 & 0 & 0 \\ 0 & 1 & 0 & -102 \\ 0 & 0 & 1 & 0 \\ 0 & 0 & 0 & 1 \end{bmatrix}$$

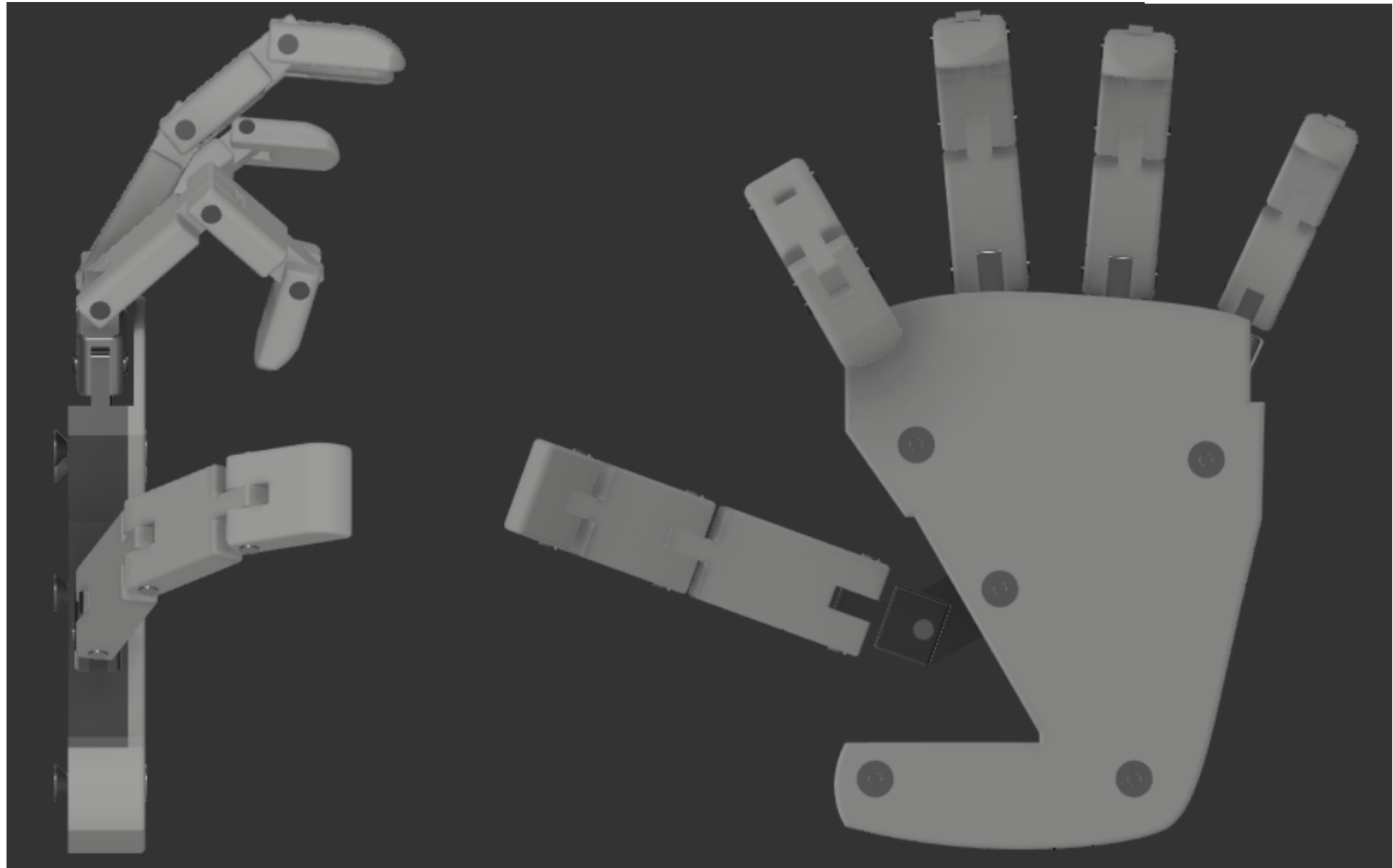
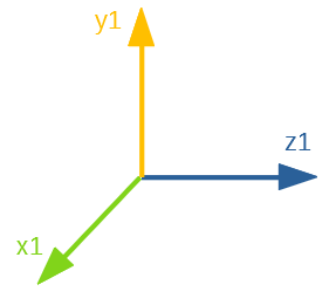
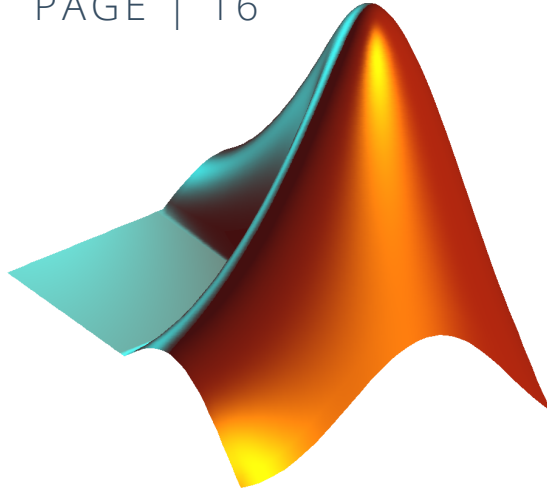
BECAUSE OF THE FACT THAT Y-ROTATION ARGUMENT IN THE FIRST JOINT HOMOGENOUS MATRIX IS EQUAL TO -1 , THE FINAL RESULT IS (-1)\*(-102MM) WHICH IS EQUAL TO 102MM .

**A1** =

$$\begin{bmatrix} 1.0000 & 0 & 0 & 0 \\ 0 & 0.0000 & -1.0000 & 0 \\ 0 & 1.0000 & 0.0000 & 0 \\ 0 & 0 & 0 & 1.0000 \end{bmatrix}$$

THE RESULTS MATCH THE REAL POSITION COORDINATES OF THE DISTAL PHALANG. THUS THE FINAL TRANSFORMATION MATRIX IS PROPERLY STRUCTURED. WE CAN MOVE FURTHER TO OBTAIN THE COORDINATES OF THE SECOND POSITION.





$T_6 =$

$$\begin{matrix} 0.8660 & 0.4830 & 0.1294 & 0.3667 \\ 0.5000 & -0.8365 & -0.2241 & -0.6352 \\ 0 & 0.2588 & -0.9659 & 37.1807 \\ 0 & 0 & 0 & 1.0000 \end{matrix}$$

$$\begin{aligned} a &= \alpha_{2\text{var}} = -45^\circ \\ b &= \alpha_{3\text{var}} = -90^\circ \\ c &= \alpha_{4\text{var}} = -60^\circ \\ d &= d_1 = 18 \text{ mm} \\ e &= d_2 = 34 \text{ mm} \\ f &= d_3 = 27 \text{ mm} \\ g &= d_4 = 23 \text{ mm} \\ k &= \theta_{1\text{var}} = 30^\circ \end{aligned}$$

THE SECOND POSITION OF THE DISTAL PHALANG OF THE SECOND FINGER  
REPRESENTED IN THE 3D CARTESIAN SYSTEM RESPECTIVELY TO THE LOCATION OF  
THE ORIGINAL COORDINATE SYSTEM:

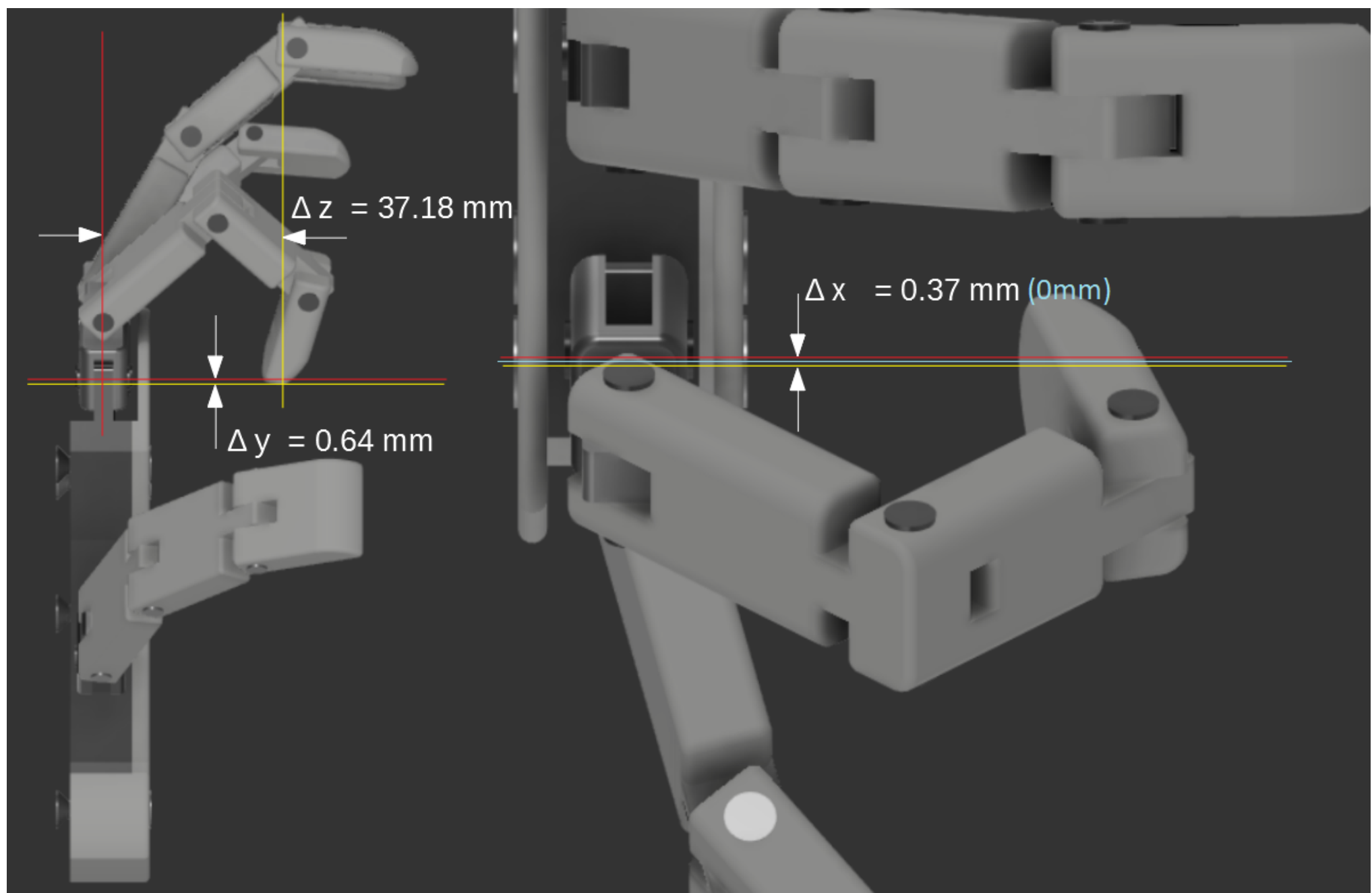
$$X = 0.37 \text{ MM}$$

$$Y = 0.64 \text{ MM}$$

$$Z = 37.18 \text{ MM}$$

BECAUSE OF THE FACT THAT Y-ROTATION ARGUMENT IN THE MCP JOINT'S  
HOMOGENOUS MATRIX IS EQUAL TO -1 , THE REAL Y-COORDINATE IS (-1)\*  
(-0.64MM), WHICH IS EQUAL TO 0.64 MM.

(THE SAME PROCEDURE AS IN FIRST POSITION IN ORDER TO GET THE POSITION  
IN REFERENCE TO THE SAME, ORIGINAL COORDINATE SYSTEM)



SIDE VIEW

TOP VIEW

$T_6 =$

$$\begin{matrix} 0.8660 & 0.4830 & 0.1294 & 0.3667 \\ 0.5000 & -0.8365 & -0.2241 & -0.6352 \\ 0 & 0.2588 & -0.9659 & 37.1807 \\ 0 & 0 & 0 & 1.0000 \end{matrix}$$

$$\begin{aligned} a &= \alpha_{2\text{var}} = -45^\circ \\ b &= \alpha_{3\text{var}} = -90^\circ \\ c &= \alpha_{4\text{var}} = -60^\circ \\ d &= d_1 = 18 \text{ mm} \\ e &= d_2 = 34 \text{ mm} \\ f &= d_3 = 27 \text{ mm} \\ g &= d_4 = 23 \text{ mm} \\ k &= \theta_{1\text{var}} = 30^\circ \end{aligned}$$

PICTURE ABOVE SHOWS THE MODEL AND THE DISPLACEMENT OF THE SECOND FINGER DISTAL PHALANG RESPECTIVELY TO THE MCP JOINT , WHICH IS THE ORIGIN OF THE WHOLE SECOND FINGER SYSTEM.

THUS WE DON'T HAVE ANY 3DOF LINK IN OUR CHAIN , THERE IS SUPPOSED TO BE NO DISPLACEMENT ABOUT THE X-AXIS , WHICH IS OBVIOUSLY A CALCULATION ERROR. THE REASON FOR THAT IS PROBABLY THE FACT , THAT EVEN THOUGH THE DISTAL PHALANG ROTATES BY  $60^\circ$  IN RESPECT TO THE DIP JOINT, THEN IN RESPECT TO ORIGINAL FRAME AND CONSIDERING THE X-AXIS , THE ANGLE IS  $75^\circ$ .

$30^\circ$ ,  $45^\circ$  AND  $90^\circ$  CAN BE VERY EASILY SIMPLIFIED DURING THE CALCULATIONS ( BASIC TRYGONOMETRIC VALUES CHART ) , WHILE  $75^\circ$  HAS BEEN ROUNDED TO THE 4TH DECIMAL PLACE, WHICH MAY BE A REASON THAT THE X-DISPLACEMENT IS NONZERO.

$$\begin{aligned} \Delta X &= 0 \text{ MM} \\ \Delta Y &= 0.64 \text{ MM} \\ \Delta Z &= 37.18 \text{ MM} \end{aligned}$$

MATRICES BELOW WERE OBTAINED IN FORWARD KINEMATICS USING DENAVIT-HARTENBERG METHOD.

IN ORDER TO CALCULATE THE INVERSE KINEMATICS FOR POSITION 1 ,  
I HAD TO PREPARE THE SYSTEM OF 3 EQUATIONS FROM FINAL  
TRANSFORMATION MATRICES

$$T_{6,0}=T_6$$

$$T_{6,0} =$$

$$\begin{pmatrix} \cos(k) & \frac{-\sin(a+b+c+k) + \sin(a+b+c-k)}{2} & \frac{-\cos(a+b+c+k) + \cos(a+b+c-k)}{2} & \frac{2 \times d \times \sin(k) + e \times \sin(a+k) + f \times \sin(a+b+k) + g \times \sin(a+b+c+k) - e \times \sin(a-k) - f \times \sin(a+b-k) - g \times \sin(a+b+c-k)}{2} \\ \sin(k) & \frac{\cos(a+b+c+k) + \cos(a+b+c-k)}{2} & \frac{-\sin(a+b+c+k) - \sin(a+b+c-k)}{2} & \frac{-2 \times d \times \cos(k) - e \times \cos(a+k) - f \times \cos(a+b+k) - g \times \cos(a+b+c+k) - e \times \cos(a-k) - f \times \cos(a+b-k) - g \times \cos(a+b+c-k)}{2} \\ 0 & \sin(a+b+c) & \cos(a+b+c) & -e \times \sin(a) - f \times \sin(a+b) - g \times \sin(a+b+c) \\ 0 & 0 & 0 & 1 \end{pmatrix}$$

$$T_6 =$$

$$\begin{pmatrix} 1 & 0 & 0 & 0 \\ 0 & 1 & 0 & -102 \\ 0 & 0 & 1 & 0 \\ 0 & 0 & 0 & 1 \end{pmatrix}$$

Sufficient condition:

$a, b, c \in [-90^\circ, -60^\circ, -45^\circ, -30^\circ, 0^\circ]$  and  $k \in [-90^\circ, -60^\circ, -45^\circ, -30^\circ, 0^\circ, 30^\circ, 45^\circ, 60^\circ, 90^\circ]$   
and  $d = 18 \text{ mm}$ ,  $e = 34 \text{ mm}$ ,  $f = 27 \text{ mm}$ ,  $g = 23 \text{ mm}$

#### **z-position**

$$\begin{aligned} -e \cdot \sin(a) - f \cdot \sin(a+b) - g \cdot \sin(a+b+c) &= 0 \\ -34 \cdot \sin(a) - 27 \cdot \sin(a+b) - 23 \cdot \sin(a+b+c) &= 0 \end{aligned}$$

$$\begin{aligned} -34 \cdot \sin(a) = 0 \Rightarrow \sin(a) = 0 &\Leftrightarrow a = 0^\circ \vee a = -180^\circ \vee a = 180^\circ \Rightarrow a = 0^\circ \\ -27 \cdot \sin(a+b) = 0 \Rightarrow \sin(a+b) = \sin(0+b) = 0 &\Leftrightarrow b = 0^\circ \vee b = -180^\circ \vee b = 180^\circ \Rightarrow b = 0^\circ \\ -23 \cdot \sin(a+b+c) = 0 \Rightarrow \sin(0+0+c) = 0 &\Leftrightarrow c = 0^\circ \vee c = -180^\circ \vee c = 180^\circ \Rightarrow c = 0^\circ \end{aligned}$$

#### **x-position**

$$d \cdot \sin(k) + 0.5 \cdot e \cdot \sin(a+k) + 0.5 \cdot f \cdot \sin(a+b+k) + 0.5 \cdot g \cdot \sin(a+b+c+k) - 0.5 \cdot e \cdot \sin(a-k) - 0.5 \cdot f \cdot \sin(a+b-k) - 0.5 \cdot g \cdot \sin(a+b+c-k) = 0$$

$$18 \cdot \sin(k) + 0.5[34 \cdot \sin(0+k) + 27 \cdot \sin(0+k) + 23 \cdot \sin(0+0+0+k) - 34 \cdot \sin(0-k) - 27 \cdot \sin(0+0-k) - 23 \cdot \sin(0+0+0-k)] = 0$$

$$18 \cdot \sin(k) + 0.5[34(\sin(k) - \sin(-k)) + 27 \cdot (\sin(k) - \sin(-k)) + 23 \cdot (\sin(k) - \sin(-k))] = 0$$

Assuming  $\sin(k) - \sin(-k) = 2\sin(k)$

$$18 \cdot \sin(k) + 0.5[68 \cdot \sin(k) + 54 \cdot \sin(k) + 46 \cdot \sin(k)] = 102 \cdot \sin(k) = 0 \Leftrightarrow \sin(k) = 0 \Rightarrow a = 0^\circ \vee k = -180^\circ \vee k = 180^\circ \Rightarrow k = 0^\circ$$

#### **y-position**

$$-18 \cdot \cos(k) - 0.5 \cdot 34 \cdot \cos(a+k) - 0.5 \cdot 27 \cdot \cos(a+b+k) - 0.5 \cdot 23 \cdot \cos(a+b+c+k) - 0.5 \cdot 34 \cdot \cos(a-k) - 0.5 \cdot 27 \cdot \cos(a+b-k) - 0.5 \cdot 23 \cdot \cos(a+b+c-k) = -102$$

$$-18 \cdot \cos(k) - 0.5[34 \cdot (\cos(k) + \cos(-k)) + 27 \cdot (\cos(k) - \cos(-k)) + 23 \cdot (\cos(k) - \cos(-k))] = -102$$

Assuming  $\cos(k) - \cos(-k) = 2\cos(k)$

$$-102\cos(k) = -102 \Leftrightarrow \cos(k) = 1 \Rightarrow k = 0^\circ$$

#### **Results for Position 1**

$$a = 0^\circ, b = 0^\circ, c = 0^\circ, k = 0^\circ$$

THE INVERSE KINEMATICS METHOD SHOWS THAT AGAIN, THE FINAL TRANSFORMATION MATRIX IS CORRECTLY CALCULATED.



IN ORDER TO CALCULATE THE INVERSE KINEMATICS FOR POSITION 2 ,  
I HAD TO PREPARE THE EQUATIONS FROM FINAL TRANSFORMATION MATRICES  
 $T_{6,0}=T_6$

$T_{6,0} =$

$$\begin{pmatrix} \cos(k) & \frac{-\sin(a+b+c+k) + \sin(a+b+c-k)}{2} & \frac{-\cos(a+b+c+k) + \cos(a+b+c-k)}{2} & \frac{2 \times d \times \sin(k) + e \times \sin(a+k) + f \times \sin(a+b+k) + g \times \sin(a+b+c+k) - e \times \sin(a-k) - f \times \sin(a+b-k) - g \times \sin(a+b+c-k)}{2} \\ \sin(k) & \frac{\cos(a+b+c+k) + \cos(a+b+c-k)}{2} & \frac{-\sin(a+b+c+k) - \sin(a+b+c-k)}{2} & \frac{-2 \times d \times \cos(k) - e \times \cos(a+k) - f \times \cos(a+b+k) - g \times \cos(a+b+c+k) - e \times \cos(a-k) - f \times \cos(a+b-k) - g \times \cos(a+b+c-k)}{2} \\ 0 & \sin(a+b+c) & \cos(a+b+c) & -e \times \sin(a) - f \times \sin(a+b) - g \times \sin(a+b+c) \\ 0 & 0 & 0 & 1 \end{pmatrix}$$

$T_6 =$

$$\begin{pmatrix} 0.8660 & 0.4830 & 0.1294 & 0.3667 \\ 0.5000 & -0.8365 & -0.2241 & -0.6352 \\ 0 & 0.2588 & -0.9659 & 37.1807 \\ 0 & 0 & 0 & 1.0000 \end{pmatrix}$$

FOR THAT COMPLEX EXAMPLE I HAD TO SOLVE THE SYSTEM OF 11 EQUATIONS :

Sufficient condition:

$a,b,c \in [-90^\circ, -60^\circ, -45^\circ, -30^\circ, 0^\circ]$  and  $k \in [-90^\circ, -60^\circ, -45^\circ, -30^\circ, 0^\circ, 30^\circ, 45^\circ, 60^\circ, 90^\circ]$   
and  $d = 18 \text{ mm}$ ,  $e = 34 \text{ mm}$ ,  $f = 27 \text{ mm}$ ,  $g = 23 \text{ mm}$

$$\cos(k)=0.866$$

$$\sin(k)=0.5$$

$$k=30^\circ$$

$$-0.5 \cdot \sin(a+b+c+k) + 0.5 \cdot \sin(a+b+c-k) = 0.4830$$

$$0.5 \cdot \cos(a+b+c+k) + 0.5 \cdot \cos(a+b+c-k) = -0.8365$$

$$-0.5 \cdot \cos(a+b+c+k) + 0.5 \cdot \cos(a+b+c-k) = -0.1294$$

$$-0.5 \cdot \sin(a+b+c+k) - 0.5 \cdot \sin(a+b+c-k) = -0.2241$$

$$\sin(a+b+c) = 0.2588$$

$$\cos(a+b+c) = -0.9659$$

$a+b+c=-165^\circ$  which means that one of them must be  $-90^\circ$ , one of them must be  $-60^\circ$  and one of them must be  $-45^\circ$

$d \cdot \sin(k) + 0.5 \cdot e \cdot \sin(a+k) + 0.5 \cdot f \cdot \sin(a+b+k) + 0.5 \cdot g \cdot \sin(a+b+c+k) - 0.5 \cdot e \cdot \sin(a-k) - 0.5 \cdot f \cdot \sin(a+b-k) - 0.5 \cdot g \cdot \sin(a+b+c-k) = 0.3667$  but as I mentioned in the forward kinematics chapter, x-displacement should be 0 and that correction slightly simplified the calculations.

$$-d \cdot \cos(k) - 0.5 \cdot e \cdot \cos(a+k) - 0.5 \cdot f \cdot \cos(a+b+k) - 0.5 \cdot g \cdot \cos(a+b+c+k) - 0.5 \cdot e \cdot \cos(a-k) - 0.5 \cdot f \cdot \cos(a+b-k) - 0.5 \cdot g \cdot \cos(a+b+c-k) = -0.6352$$

$$-e \cdot \sin(a) - f \cdot \sin(a+b) - g \cdot \sin(a+b+c) = 37.1807$$

After solving above system of equations, with I obtained following results for the Position 2 :

$$\begin{aligned} \Rightarrow a &= -45^\circ \\ \Rightarrow b &= -90^\circ \\ \Rightarrow c &= -60^\circ \\ \text{and } k &= 30^\circ \end{aligned}$$

THE INVERSE KINEMATICS METHOD SHOWS THAT AGAIN, THE FINAL TRANSFORMATION MATRIX IS CORRECTLY CALCULATED.



## WHY I CHOSE THE PVC - POLYVINYLCHLORIDE AS THE MATERIAL

### DYNAMIC RESPONSE OF POLYMERS

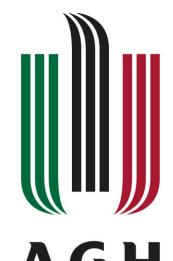
WALLEY AND FIELD (WALLEY S, FIELD J, POPE P, SAFFORD N (1989) A STUDY OF THE RAPID DEFORMATION BEHAVIOUR OF A RANGE OF POLYMERS. PHILOS TRANS R SOC LOND A MATH PHYS ENG SCI 328(1597):1-33) PUBLISHED AN EXTENSIVE SET OF DATA CHARACTERIZING THE COMPRESSIVE STRESS-STRAIN RESPONSE OVER A RANGE OF STRAIN RATES FOR A BROAD RANGE OF POLYMERS. THEY OBSERVED A RANGE OF MATERIAL RESPONSES DEPENDING ON THE POLYMER STRUCTURE.

### GLASSY AMORPHOUS POLYMERS

HERE ARE SEVERAL GLASSY POLYMERS THAT HAVE BEEN EXTENSIVELY STUDIED AT HIGH STRAIN RATE IN THE LITERATURE, INCLUDING POLYMETHYLMETHACRYLATE (PMMA), POLYCARBONATE (PC), POLYVINYLCHLORIDE (PVC) AND VARYING CLASSES OF EPOXY.

Representative compressive stress-strain curves for these materials across a range of strain rates are shown in Fig. 5, which show many similarities across the class of materials. Typically, the stress-strain curve has an initial viscoelastic behavior which becomes increasingly non-linear as strain increases until it reaches a peak stress. The peak stress is followed by strain softening and then strain hardening. Hasan and Boyce describe the stress-strain response in terms of the evolution of shear transformation sites, where the initial material has a number of sites with a probability of transformation within the timeframe of the experiment. As stress is applied to the material (viscoelastic rise), transformation sites with high local free volume and, subsequently, low activation energy begin to yield and flow, and the corresponding transformation strain energy is stored in the non-transformed "matrix," which creates a back stress that initially inhibits further transformation. With increasing stress, transformation sites with higher activation energy can be accessed resulting in increasingly non-linear stress-strain response.

The surrounding material stores the transformation strain energy, which exerts a back stress on the transformed material. As the applied stress increases, transformation sites with higher activation energy are accessed and the surrounding material can no longer absorb the transformation strain energy, which results in the creation of new defects, i.e. sites with high local free volume. These new sites result in strain softening in the material, where there are sites available to transform with lower activation energy. At this point, the material is in a steady-state condition where the mobile regions are prolific through the material allowing for indefinite plastic flow. At higher strains, resistance to polymer chain alignment causes strain hardening in the material. However, with increasing strain rate, this strain hardening effect is balanced by adiabatic heating in the material, which ultimately dominates over the hardening from resistance to polymer chain alignment. Finally, in the case of PMMA (Fig. 5a), at high strain rates the material fails catastrophically due to the inability to access particular molecular side chain motions at these fast rates.



## WHY I CHOSE THE PVC - POLYVINYLCHLORIDE AS THE MATERIAL

### DYNAMIC RESPONSE OF GLASSY AMORPHOUS POLYMERS

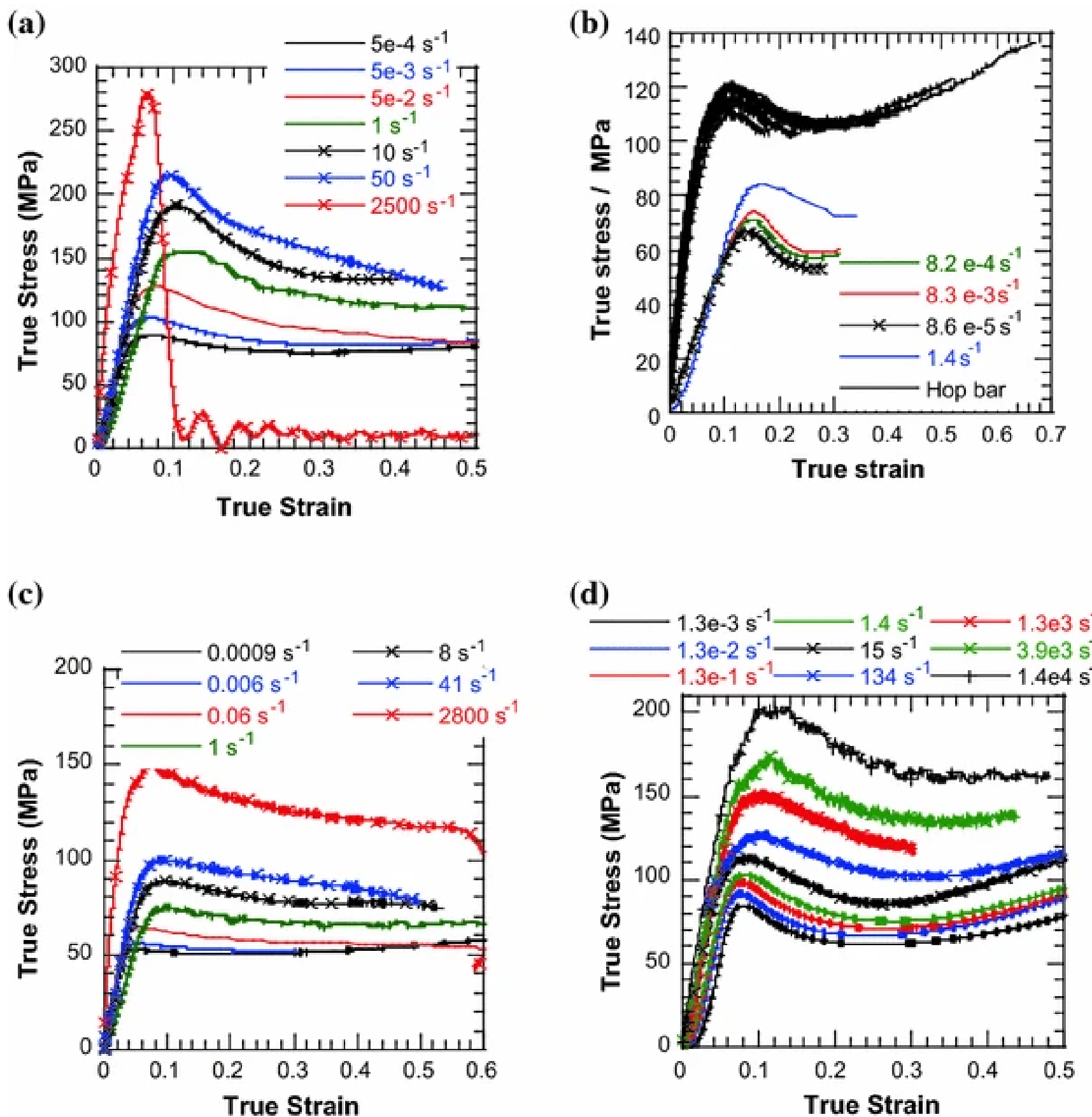


figure 5

Compressive stress-strain curves for a) polymethylmethacrylate (PMMA), b) polycarbonate (PC) , c) polyvinylchloride (PVC) , and d) varying classes of epoxy across a range of strain rates

## WHY I CHOSE THE PVC - POLYVINYLCHLORIDE AS THE MATERIAL

### DYNAMIC RESPONSE OF POLYMERS

The strain rate dependence of these polymers becomes more obvious when the peak stress is plotted versus log strain rate as shown in Fig. 6 for the same range of semi-crystalline polymers presented in Fig. 5. The most interesting observation in these materials is the increased strain rate sensitivity at higher strain rates, which has been observed in a wide variety of polymer materials, in addition to those presented. However, caution should be taken when interpreting these results for three reasons. A similar increase in strain rate sensitivity has been observed in metals, e.g. copper. Secondly, the strain rates where the increased sensitivity occurs are also those where inertial effects become relevant, i.e. if the specimen is too large, the stress induced by specimen inertia can become significant compared to the polymer strength. Finally, the transition in behavior occurs over the same regime where test equipment changes from screw-driven or hydraulic load frames to split Hopkinson pressure bars.

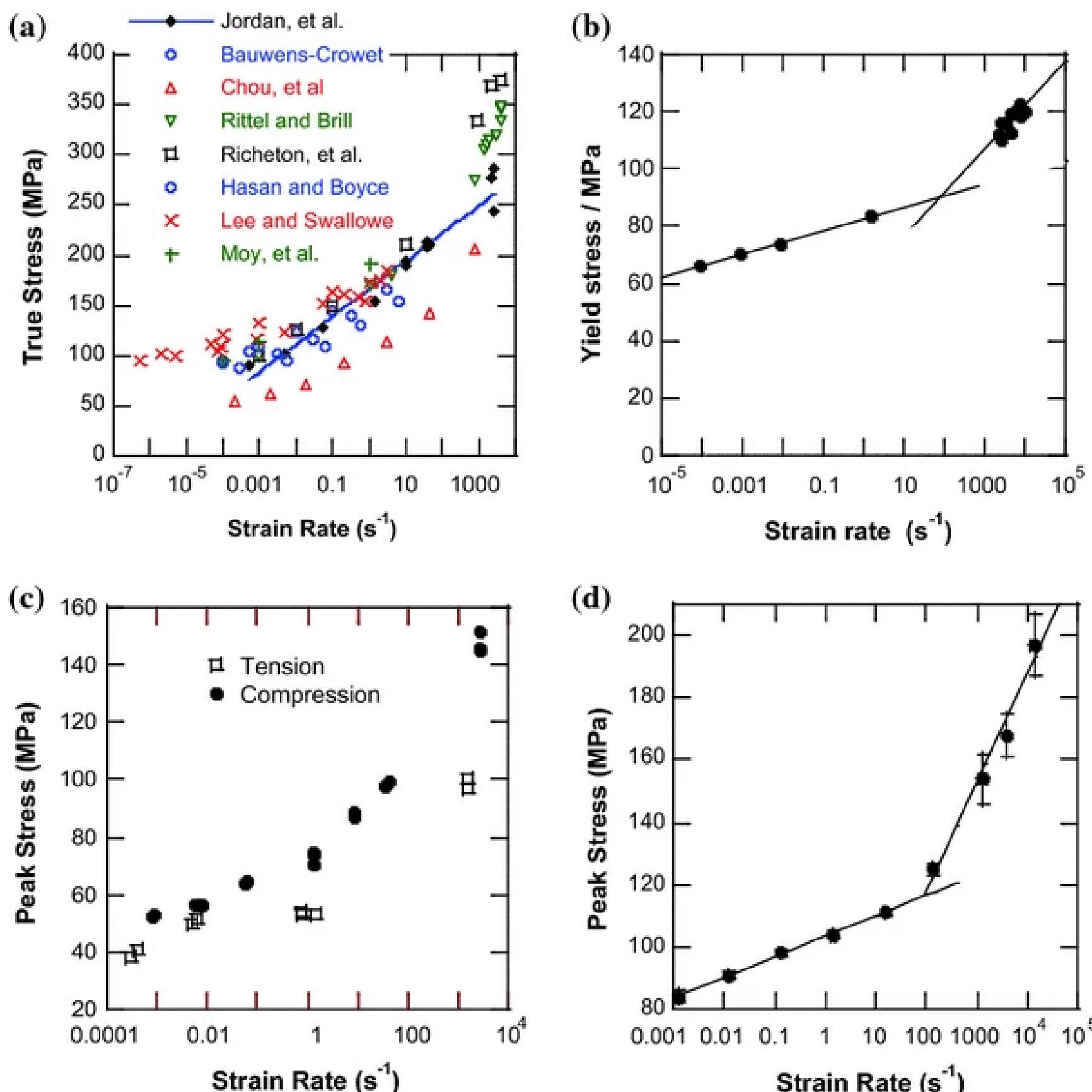


*figure 6*

Peak stress vs. strain rate for a) polymethylmethacrylate (PMMA) , b) polycarbonate (PC) , c) polyvinylchloride (PVC) , and d) variuos classes of epoxy  
across a range of strain rates

## WHY I CHOSE THE PVC - POLYVINYLCHLORIDE AS THE MATERIAL

### DYNAMIC RESPONSE OF POLYMERS

Typically, the increase in strain rate sensitivity in glassy polymers is attributed to activation of particular molecular mobility, often due to side chain motion or ring flips called the  $\beta$ -transition. There is considerable scatter between the data from different studies, as seen in Fig. 6a, again emphasizing that the polymer pedigree is important in determining the mechanical response. For polymethylmethacrylate (PMMA), which is used as a reference and window material in shock experiments, understanding the cause of these differences is critical.

Consideration of polymer processing, particularly annealing as-received or aged materials, should be done prior to experimentation.

### PRESSURE RESPONSE OF POLYMERS

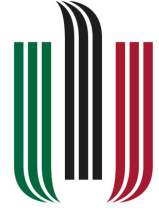
Although pressure effects can play a large role on the mechanical properties of polymers, there has been limited research into this topic, particularly recently.

The first study where a polymer was loaded under hydrostatic pressure was conducted by Bridgman in 1953. In 1975, Pae and Bhateja wrote a review of the effects of hydrostatic pressure on the mechanical behavior of polymers, including specific properties of the polymers that had been characterized to date. In their survey of materials, they found that while all polymers exhibit pressure dependent properties, some features are material specific, and some are observed across all polymers, namely that increasing hydrostatic pressure results in increased modulus and yield stress, sometimes by as much as 50–100 %. Increasing pressure in materials where the glass transition is below room temperature was found to shift the transition to room temperature, for example in low density polyethylene (LDPE), similar to time-temperature superposition. Due to the differences in underlying deformation mechanisms, the ductility and post yield behavior in polymers varies by material. The hydrostatic pressure dependence of yield in polymers has been observed by many authors. The physical manifestation of this pressure dependence is a difference in tensile and compressive yield stress for the same material, as demonstrated for polyvinylchloride (PVC) in Fig. 6c.

As shown in Table 1, these ratios are between 1 and 1.4 for a variety of polymeric materials, where a ratio of 1 indicates that the material is nominally pressure insensitive. Several yield criteria have been used to describe the yield behavior in polymers with the similarity between them being that the yield stress displays a linear dependence on hydrostatic pressure.

Material	$\sigma_C/\sigma_T$
High density polyethylene (HDPE)	1.0
	1.18
Polycarbonate (PC)	1.20
	1.11
Polypropylene (PP)	1.24
Polyvinylchloride (PVC)	1.33
	1.3

Table 1  
Ratio of compressive to tensile yield strength for a range of polymers  
From: High Strain Rate Mechanics of Polymers: A Review



## WHY I CHOSE THE PVC - POLYVINYLCHLORIDE AS THE MATERIAL

### STRONG & LIGHTWEIGHT AT THE SAME TIME

PVC's **abrasion resistance**, **light weight (1.45g/cm<sup>3</sup>)**, good **mechanical strength** and **toughness** are key technical advantages.

### SIMPLE IN MANUFACTURING & INSTALLATION

PVC can be **cut**, **shaped**, **welded** and **joined easily in a variety of styles**. Its light weight reduces manual handling difficulties.

### DURABLE

PVC is **resistant to weathering**, **chemical rotting**, **corrosion**, **shock** and **abrasion**. It is therefore the preferred choice for many different long-life and used in unfavourable conditions products.

### GREAT COST TO PERFORMANCE RATIO

PVC has great physical and technical properties which provide excellent **cost-performance** advantages. As a material it is very competitive in terms of price, this value is also enhanced by the properties such as its **durability**, **lifespan** and low **maintenance costs**.

### SAFE IN USAGE

PVC is **non-toxic**. It is a safe material and a socially valuable resource that has been used for more than half a century. It is also the world's most researched and thoroughly tested plastic. It meets all international standards for **safety** and **health** for both the products and applications for which it is used.

### HIGH TEMPERATURE & FIRE RESISTANT

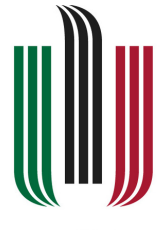
PVC products are **self-extinguishing**, i.e. if the ignition source is withdrawn they will stop burning. Because of its high chlorine content PVC products have **fire safety characteristics**, which are quite favourable as. they are **difficult to ignite**, heat production is comparatively low and they tend to char rather than generate flaming droplets

### GOOD INSULATOR

PVC **does not conduct electricity** and is therefore an excellent material to use for **electrical applications**.

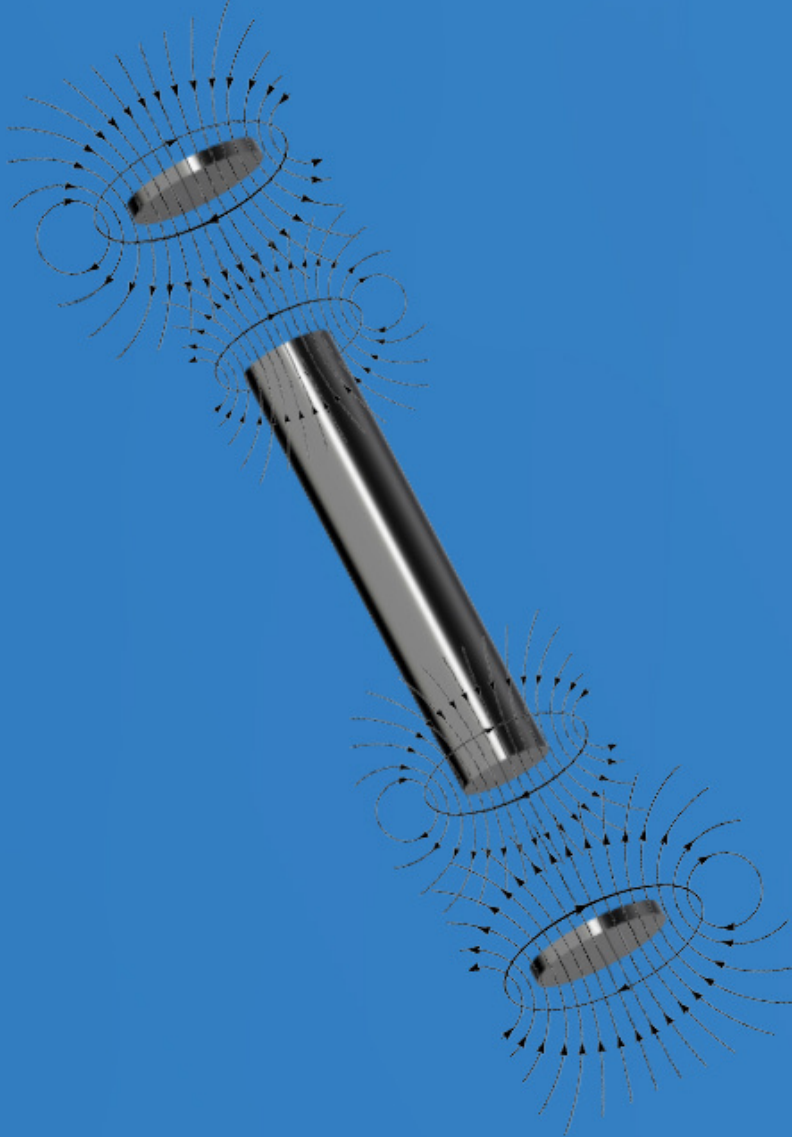
### VERSATILE

The physical properties of PVC **allow designers a high degree of freedom** when designing new products and developing solutions where PVC acts as **a replacement or refurbishment material**.



AKADEMIA GÓRNICZO-HUTNICZA  
IM. STANISŁAWA STASZICA  
W KRAKOWIE

# JOINT SPINDLE CLAMP USING MAGNETIC FIELD TECHNOLOGY



Alnico alloys were considered to be the strongest kind of magnets before rare earth magnets were developed in the 1970s. Alnico alloys have ferromagnetic properties which makes it strong permanent magnets. They are listed as some of the best permanent magnets for over fifty years now. Alnico alloys can also be magnetized to create strong magnetic fields. These magnets also show excellent stability in a wide range of temperature.

The general composition of Alnico alloys is Al- 8-12%, Ni- 15-26%, and Co- 5-24%. It may also contain up to 6% copper (Cu), and up to 1% titanium (Ti). Depending on the percentage of the different components, there can be various different types of Alnico alloys.

Based on the process of preparation, and the different uses, alnico alloys can be classified into three main types:

- **Cast Alnico**
- **Sintered Alnico**
- **Bar Alnico**

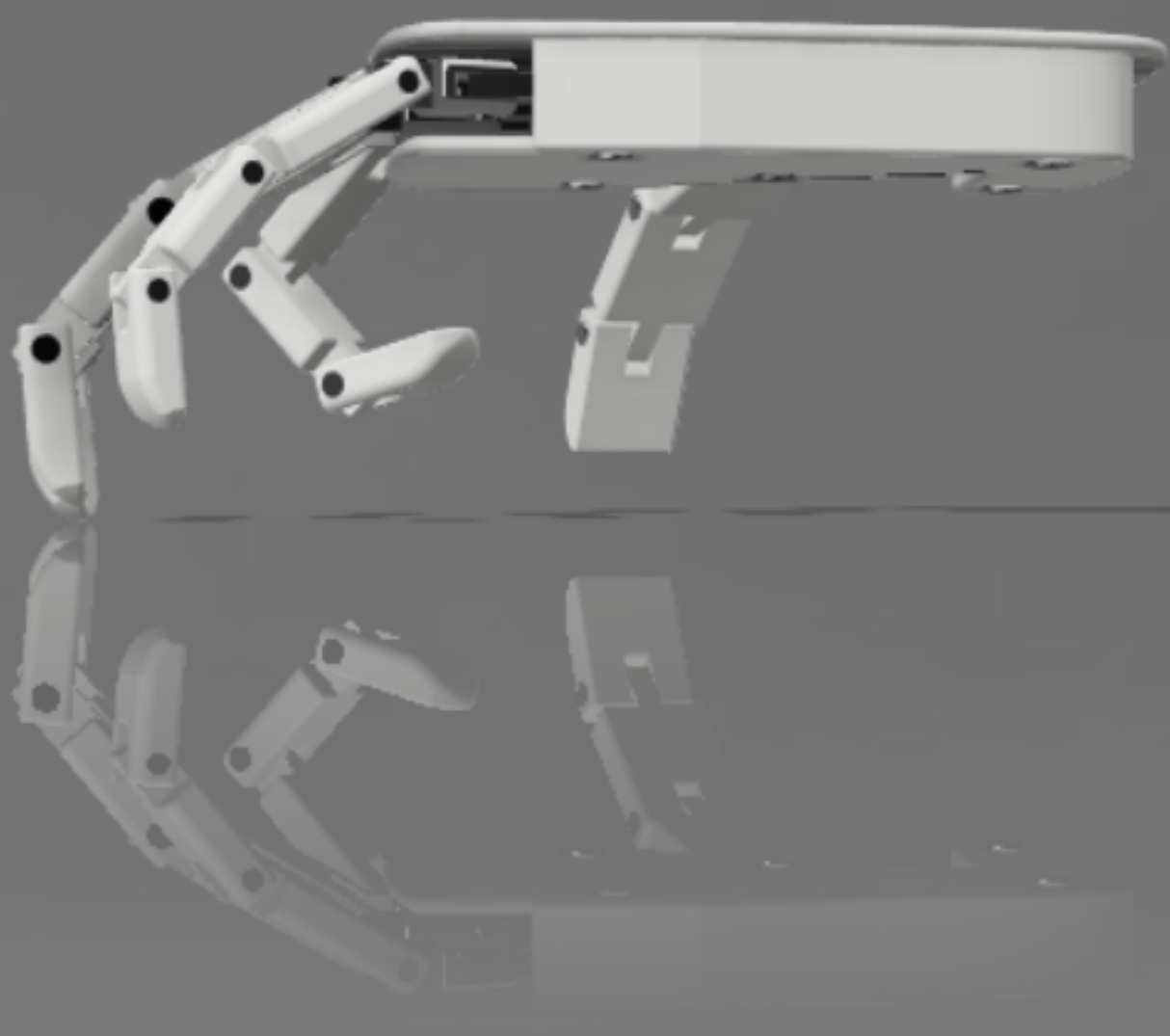
*In order to manufacture the spindle , the cast alnico is sufficient.*

- All Alnico alloys have strong magnetic properties and high ferromagnetism ,while they can be still highly efficient in the temperatures up to 540°C.
- Alnico alloys are the only magnets to have useful magnetic powers at red hot temperature (500°C – 800°C).
- Alnico magnets have some of the highest curie points among all the magnetic materials. It ranges around 800°C.
- Unlike ceramic magnets, Alnico magnets have the property of electric conductivity.
- Alnico alloys have very good resistance to corrosion.
- Some Alnico alloys can have isotropic properties while others can have anisotropic properties.

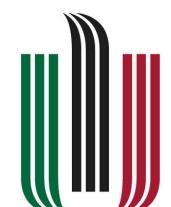


## 3D - MODEL LOOK

I'VE CREATED A HUMAN HAND PROSTHETIC MODEL IN THE  
AUTODESK FUSION 360 SOFTWARE



// PREPARED FOR SERVICE ROBOTS PROJECT

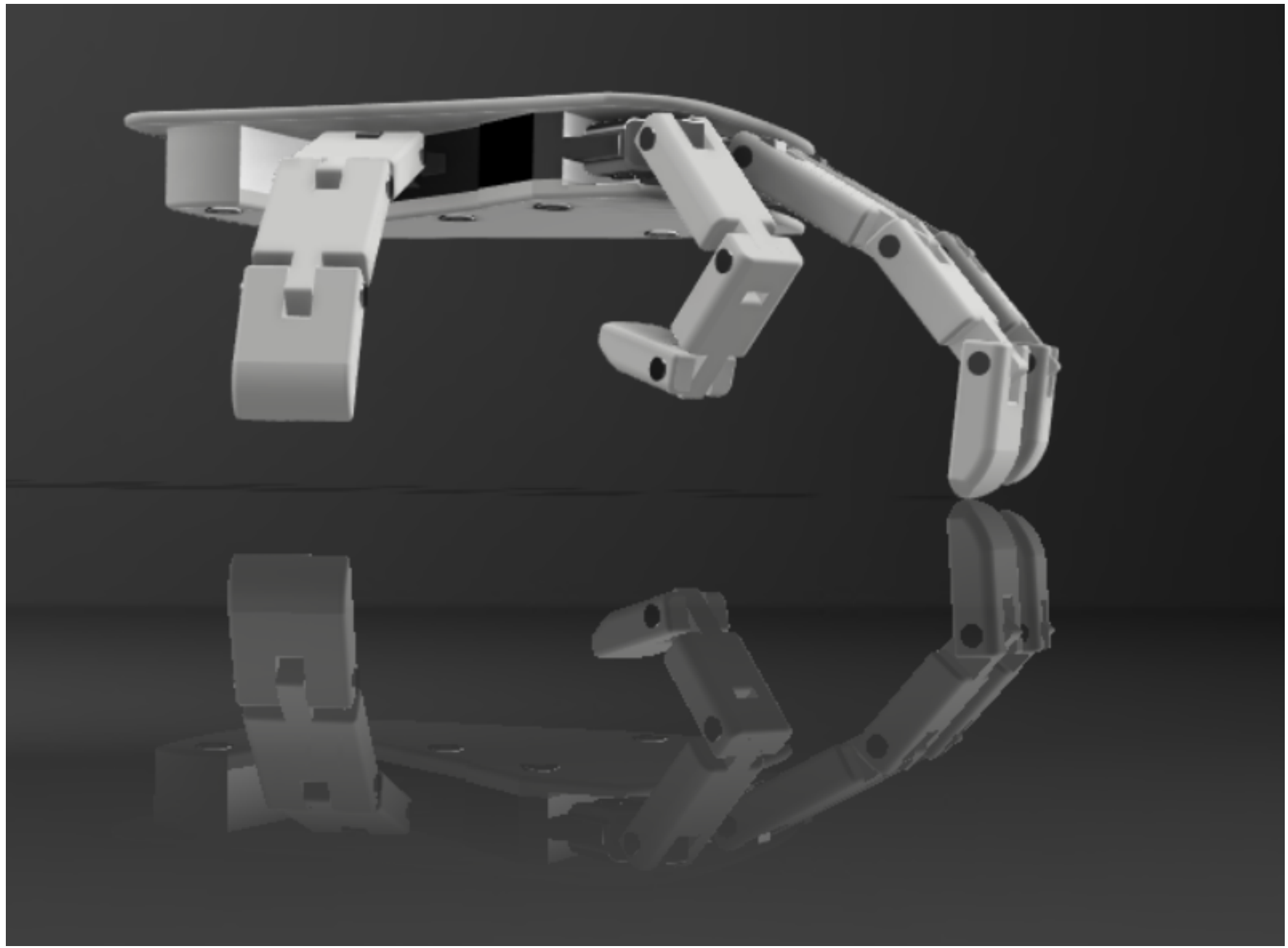
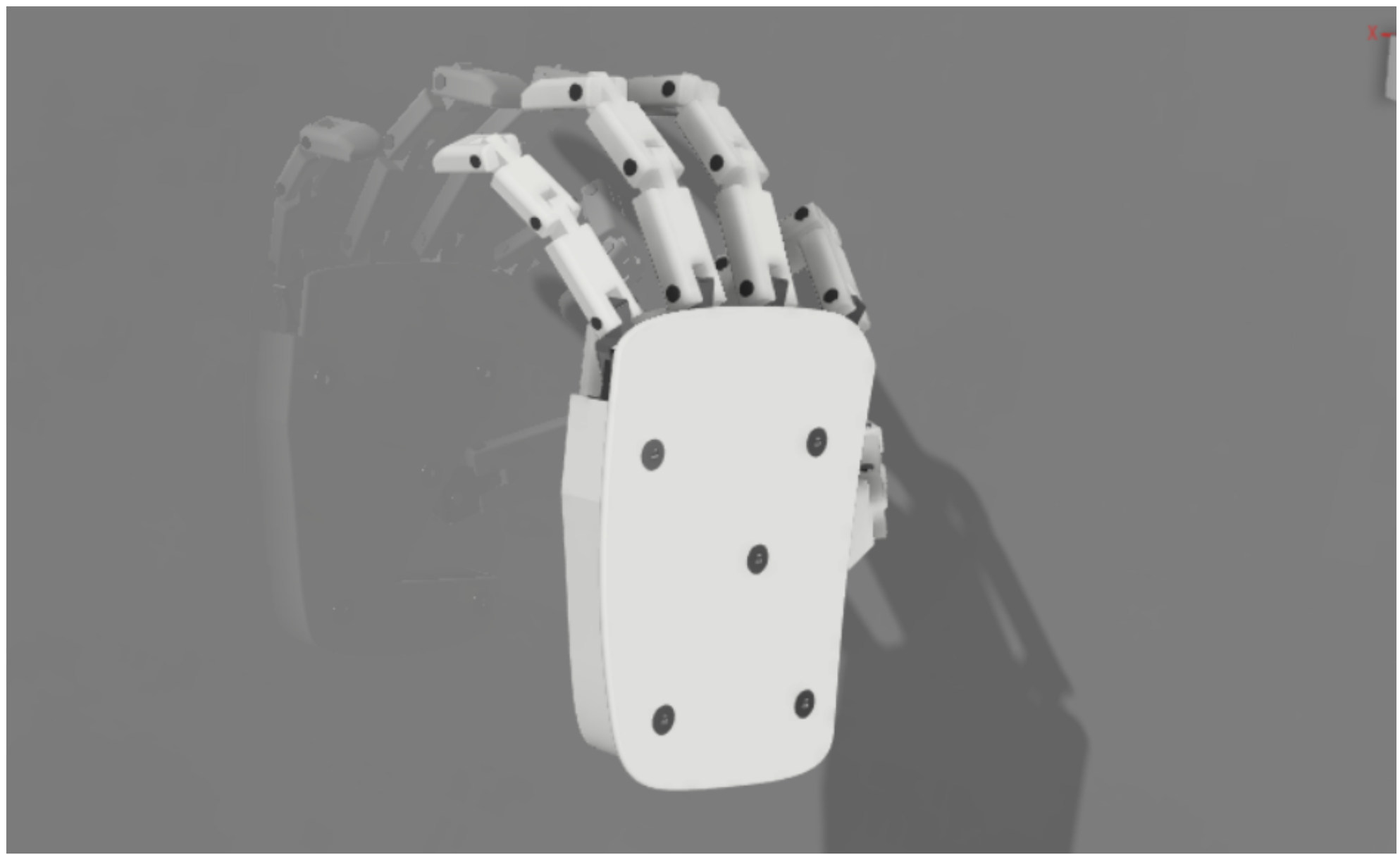


AGH

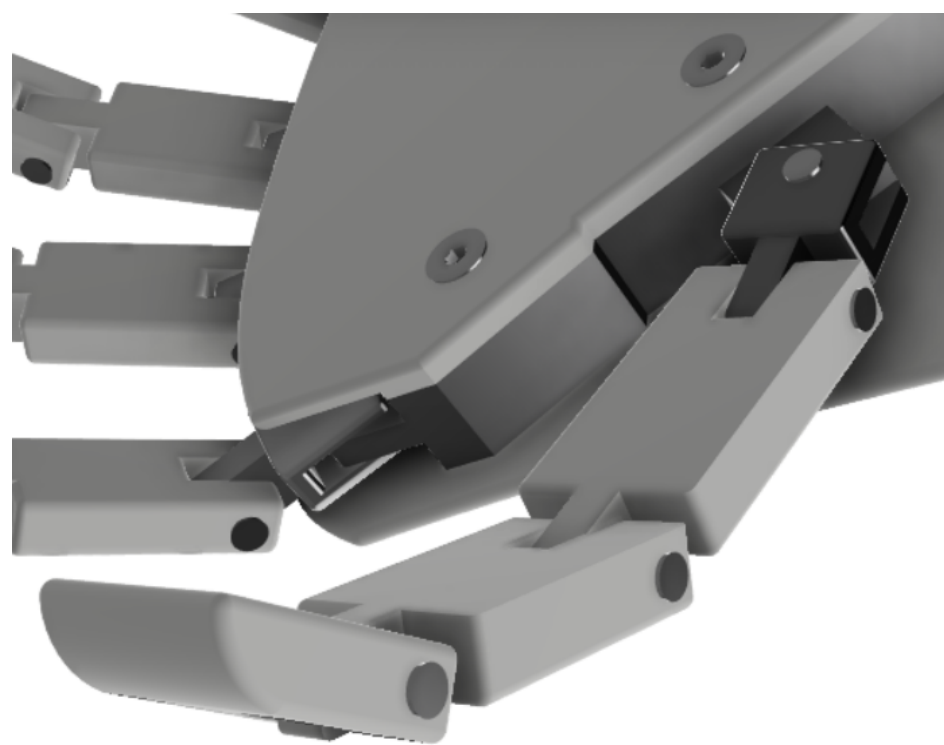
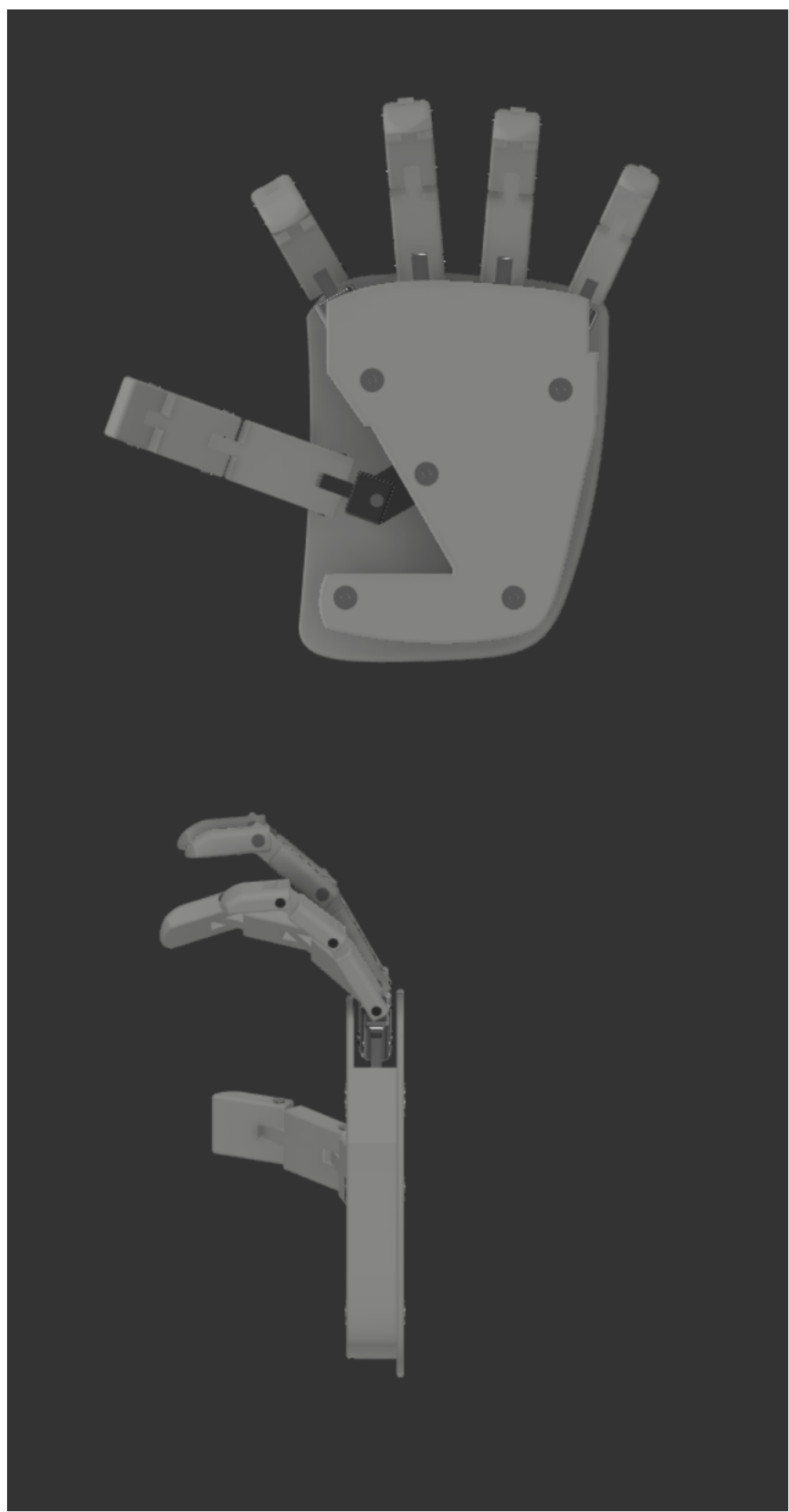
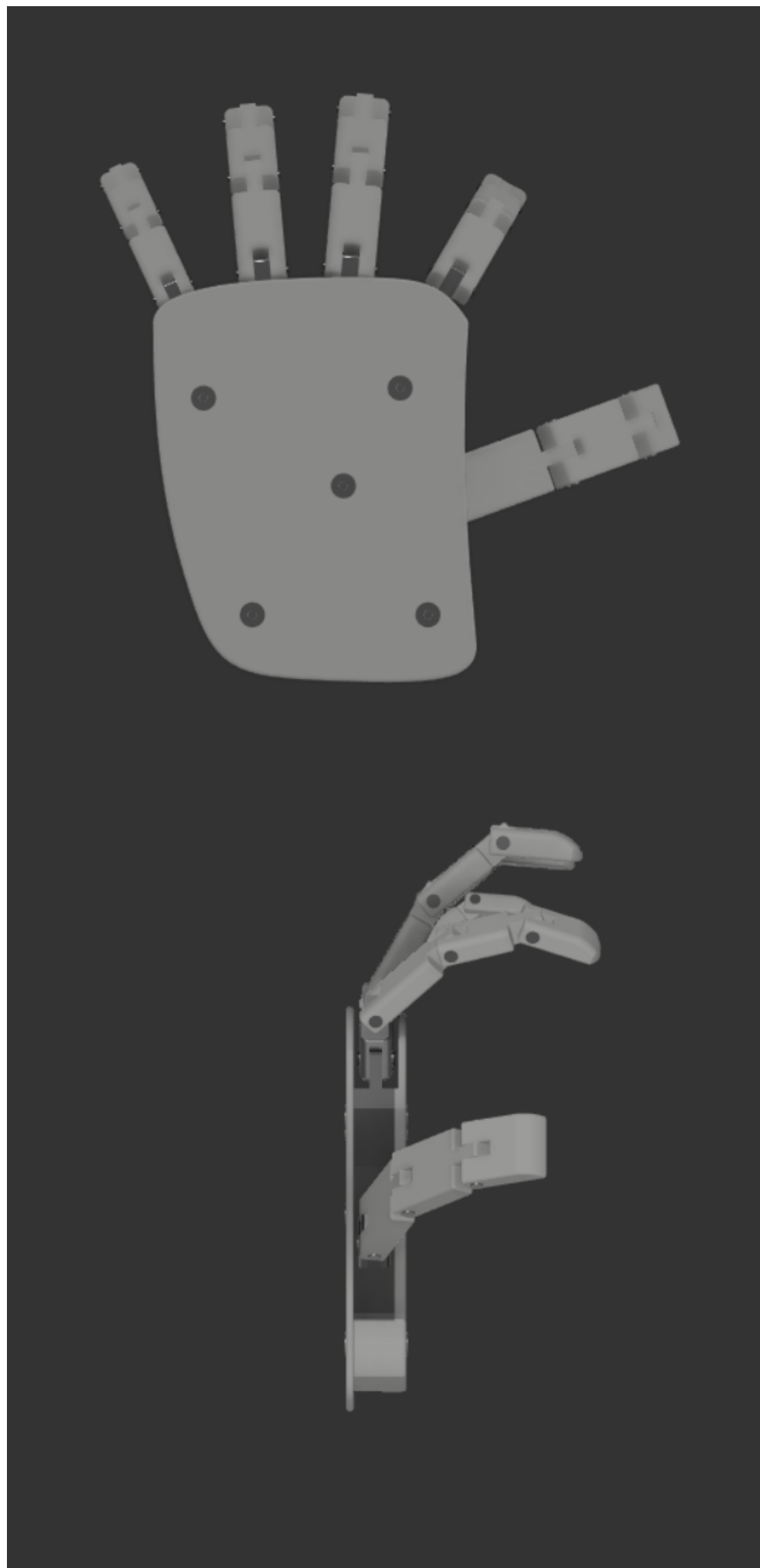
AKADEMIA GÓRNICZO-HUTNICZA  
IM. STANISŁAWA STASZICA  
W KRAKOWIE

2019-2020 // IMIR MECHATRONICS ENGINEERING

## 3D - MODEL LOOK

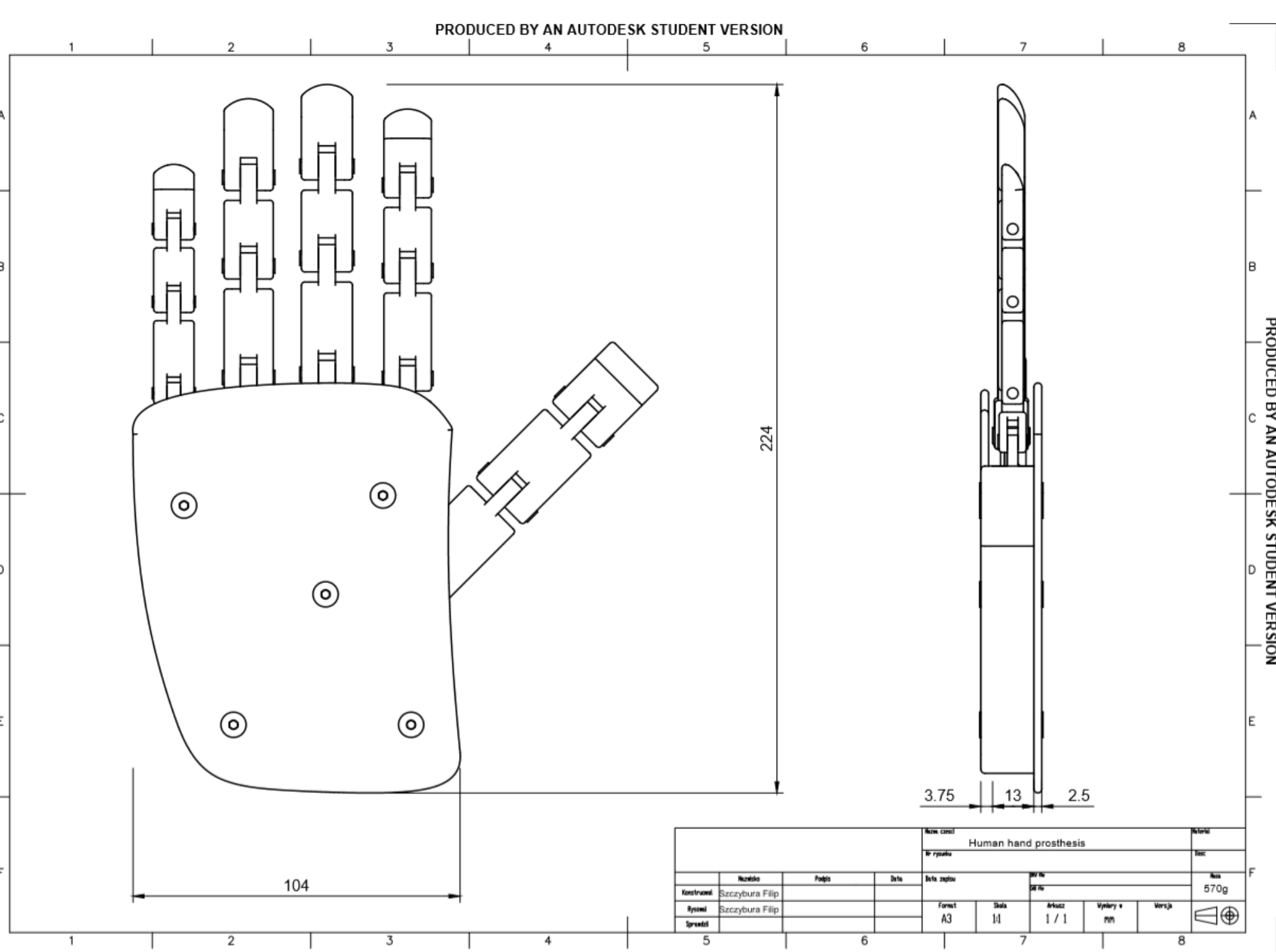
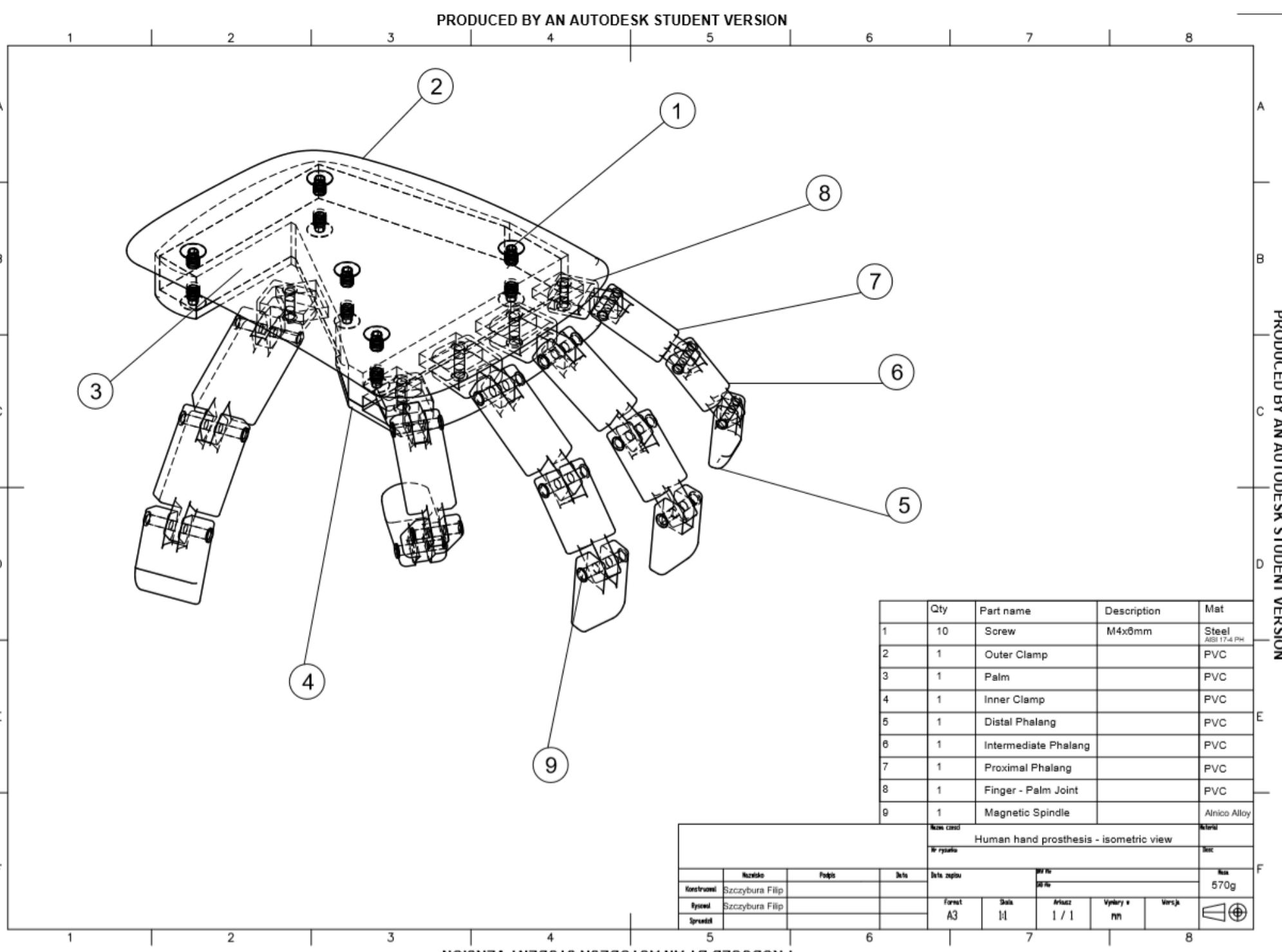


## 3D - MODEL LOOK



# 3D & 2D MODEL ASSEMBLY DRAWINGS

I GENERATED PROJECTED VIEWS IN FUSION 360 AND PREPARED THE FINAL DRAWINGS IN AUTOCAD 2019



// PREPARED FOR SERVICE ROBOTS PROJECT



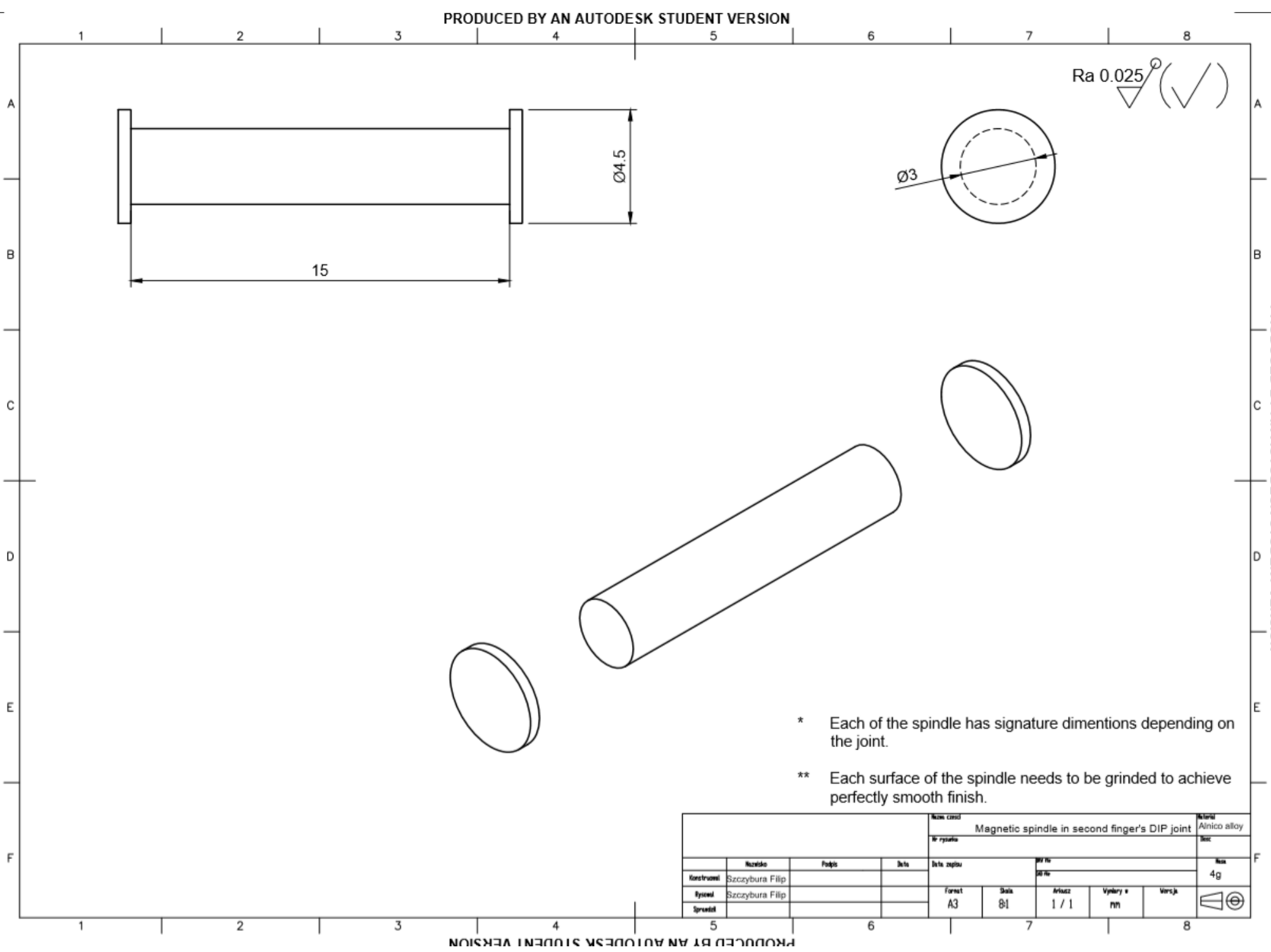
AGH

AUH  
AKADEMIA GÓRNICZO-HUTNICZA  
IM. STANISŁAWA STASZICA

# CHOSEN PARTS DRAWING - SECOND FINGER

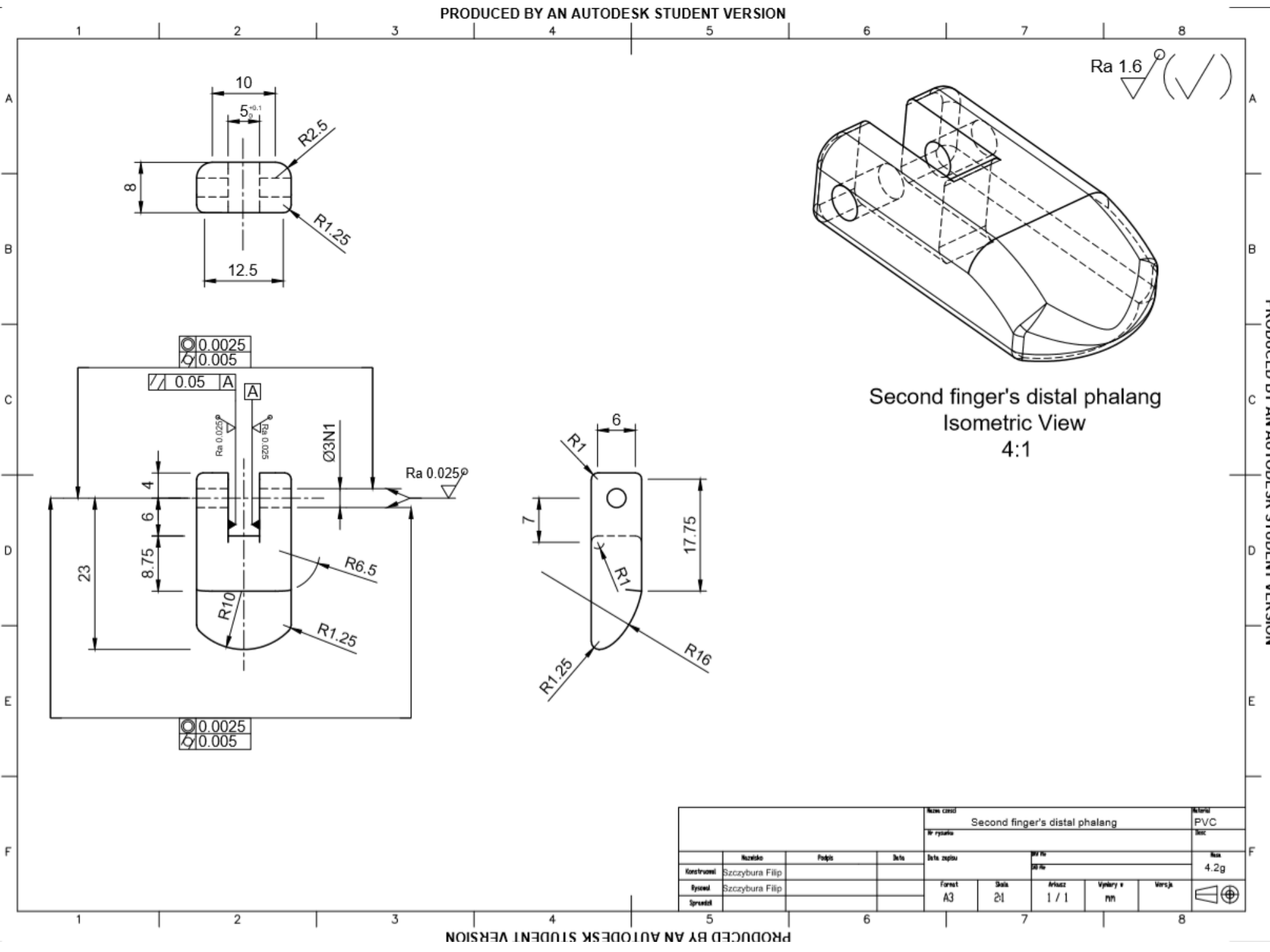
PRODUCED BY AN AUTODESK STUDENT VERSION

PRODUCED BY AN AUTODESK STUDENT VERSION



KULULEU BY AN AUTORESK SIUENI VERSIUN

PRODUCED BY AN AUTODESK STUDENT VERSION



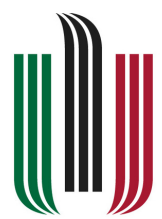
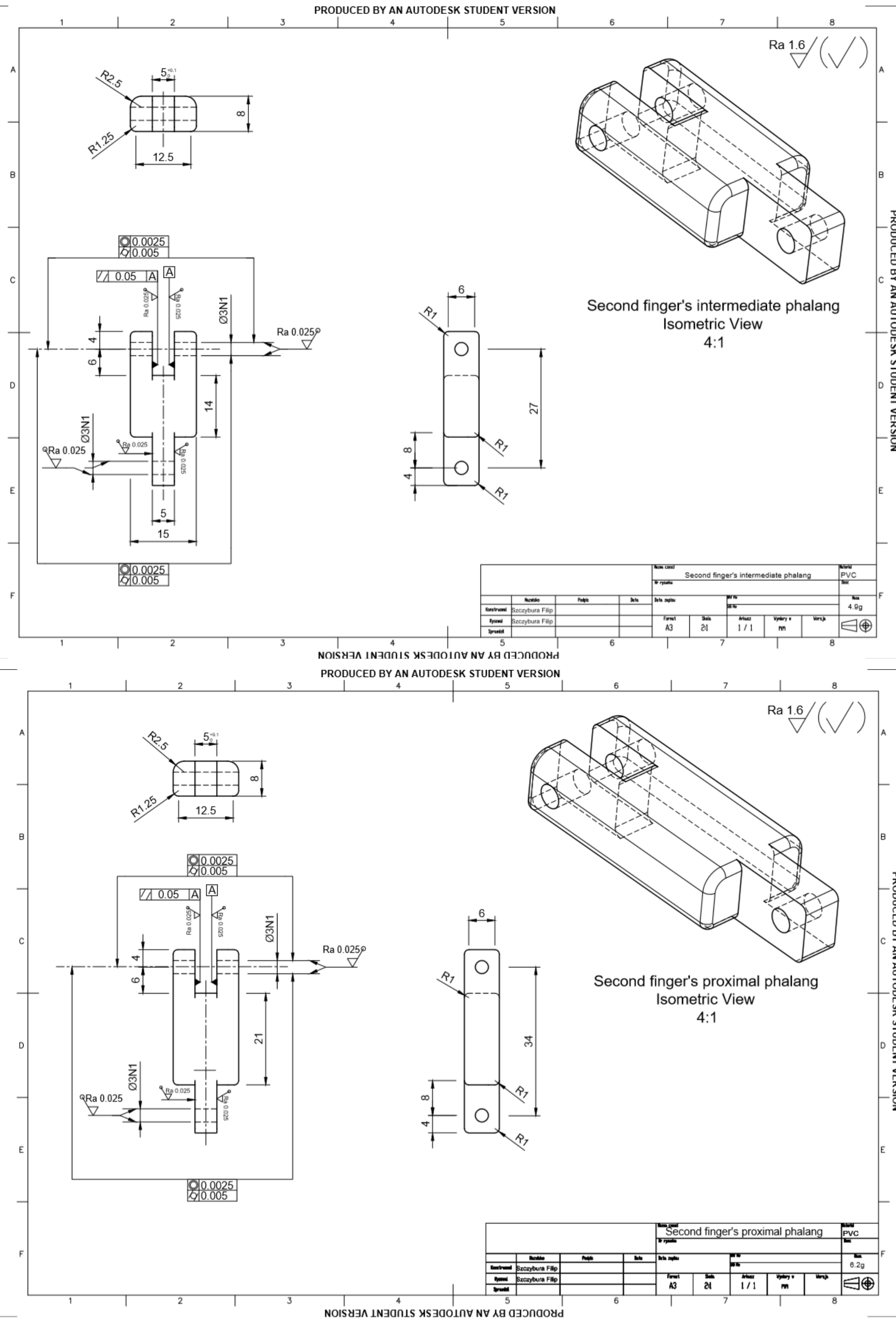
AGH

**AGH**  
AKADEMIA GÓRNICZO-HUTNICZA  
IM. STANISŁAWA STASZICA  
W KRAKOWIE

// PREPARED FOR SERVICE ROBOTS PROJECT

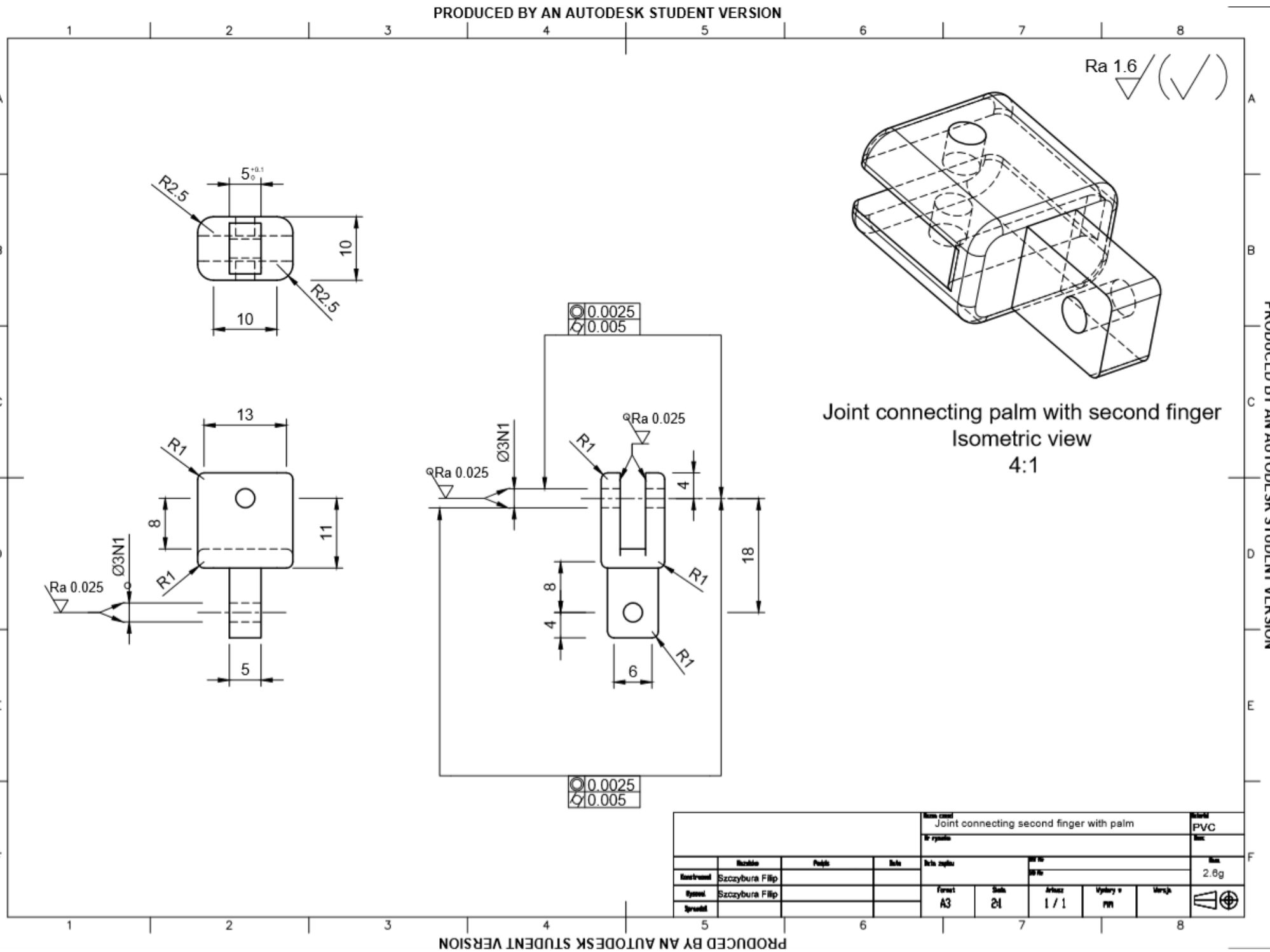
2019-2020 // IMIR MECHATRONICS ENGINEERING

## CHOSEN PARTS DRAWING - SECOND FINGER

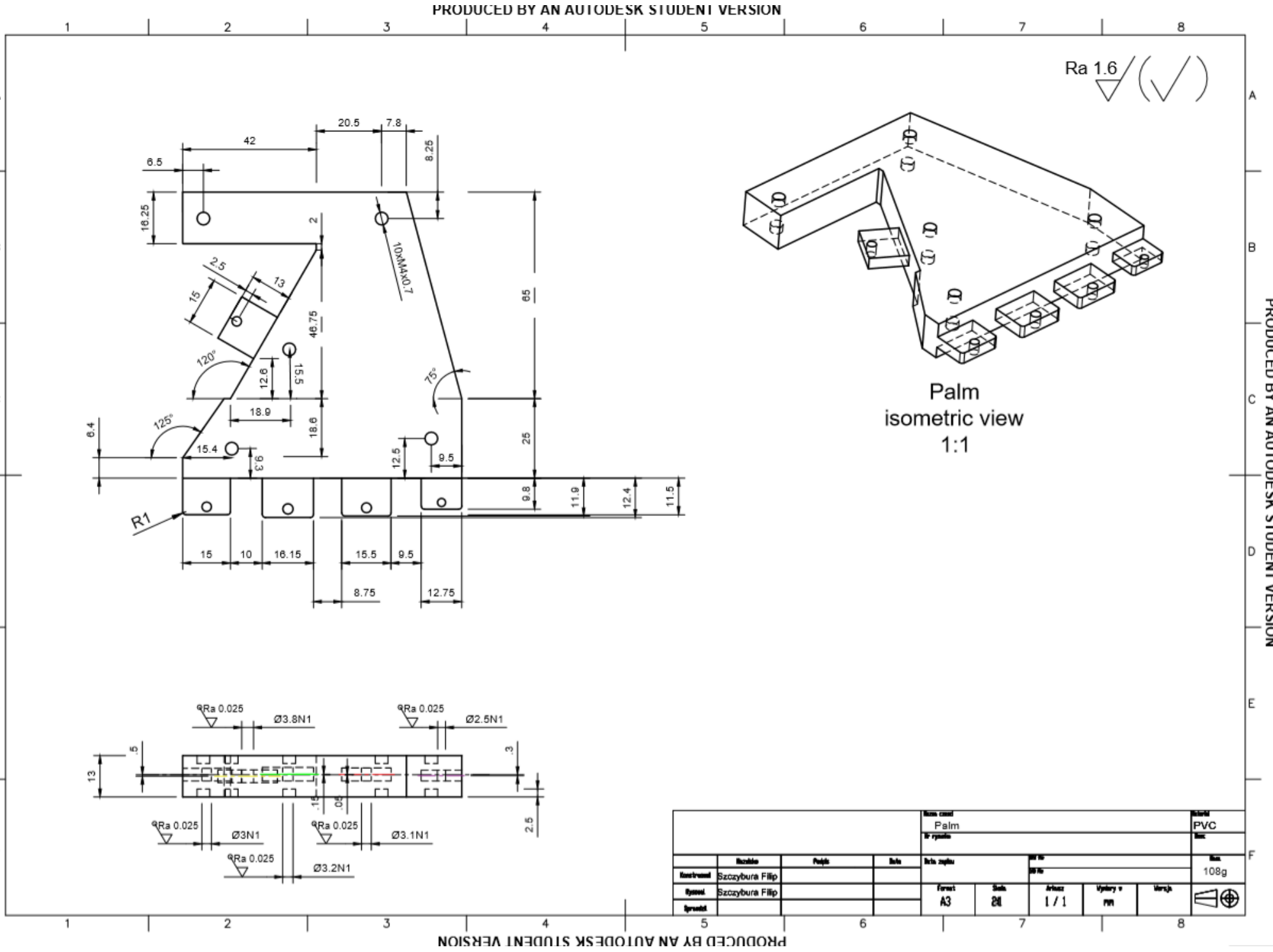


## CHOSEN PARTS DRAWING - SECOND FINGER

PRODUCED BY AN AUTODESK STUDENT VERSION

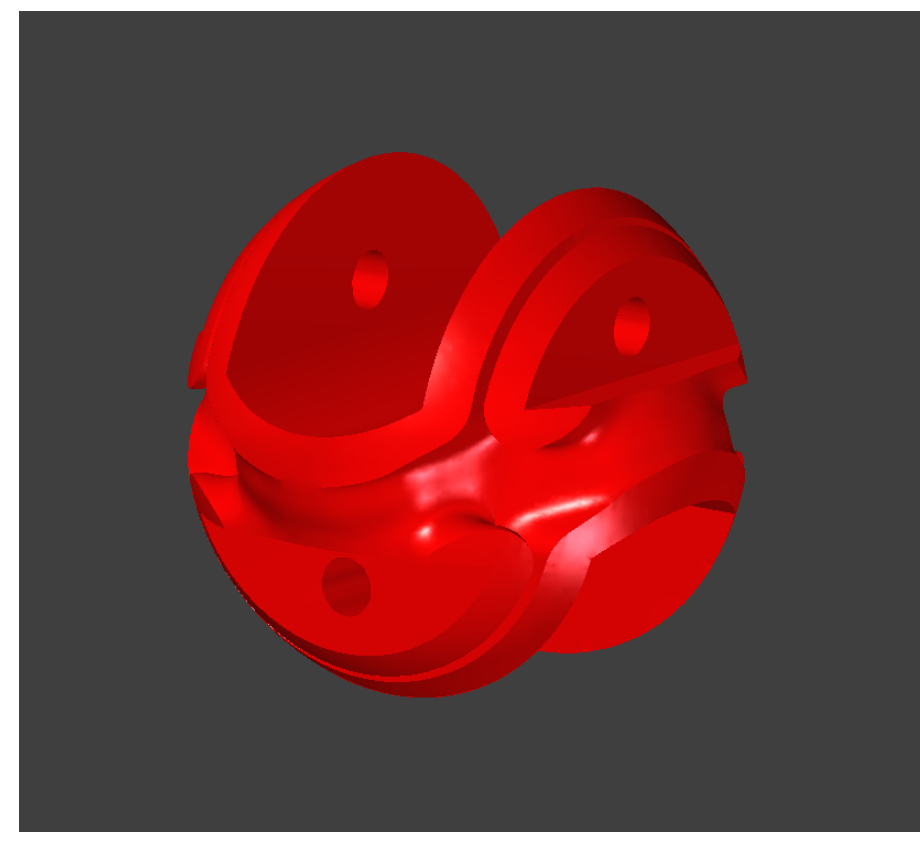
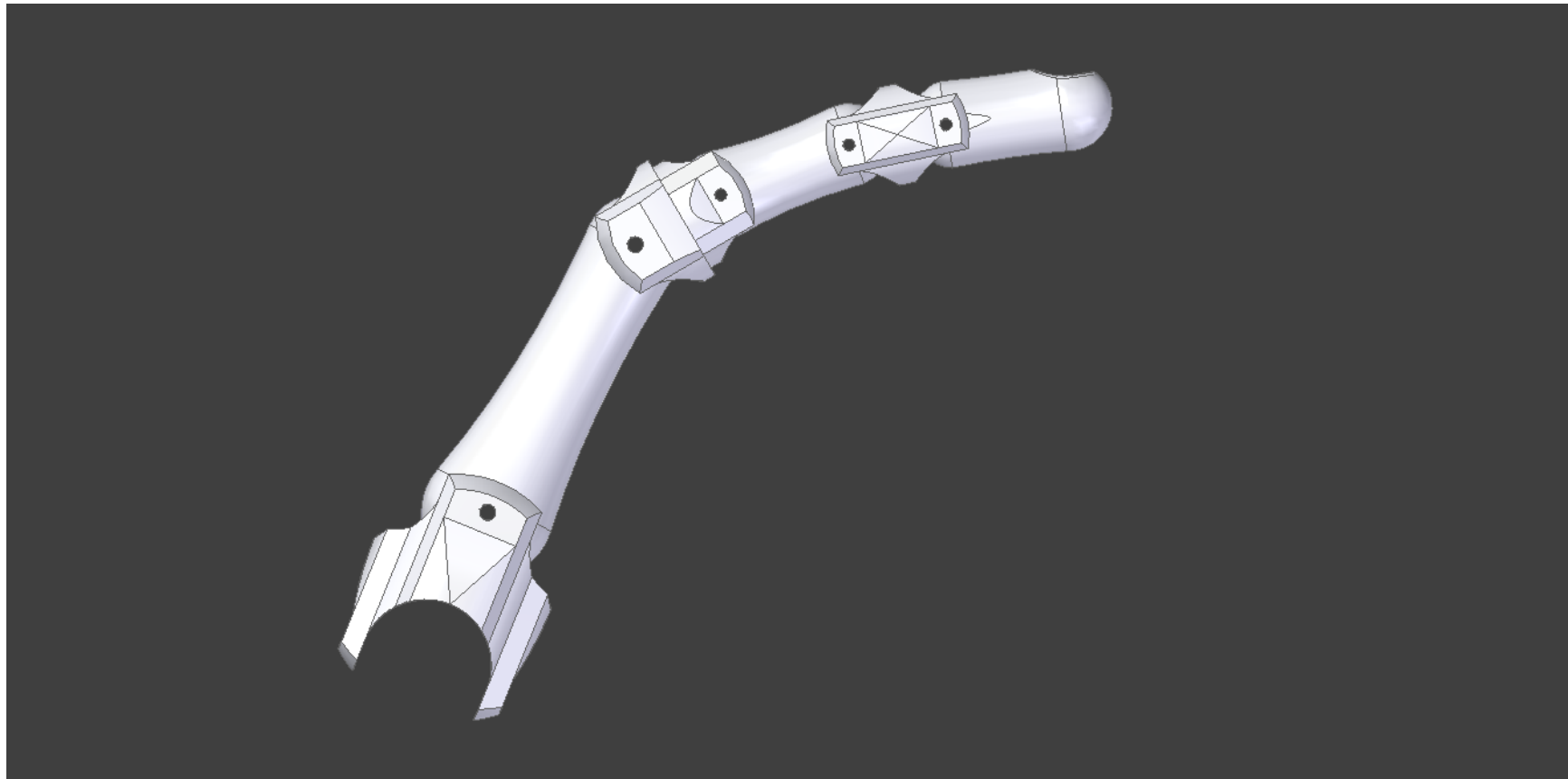
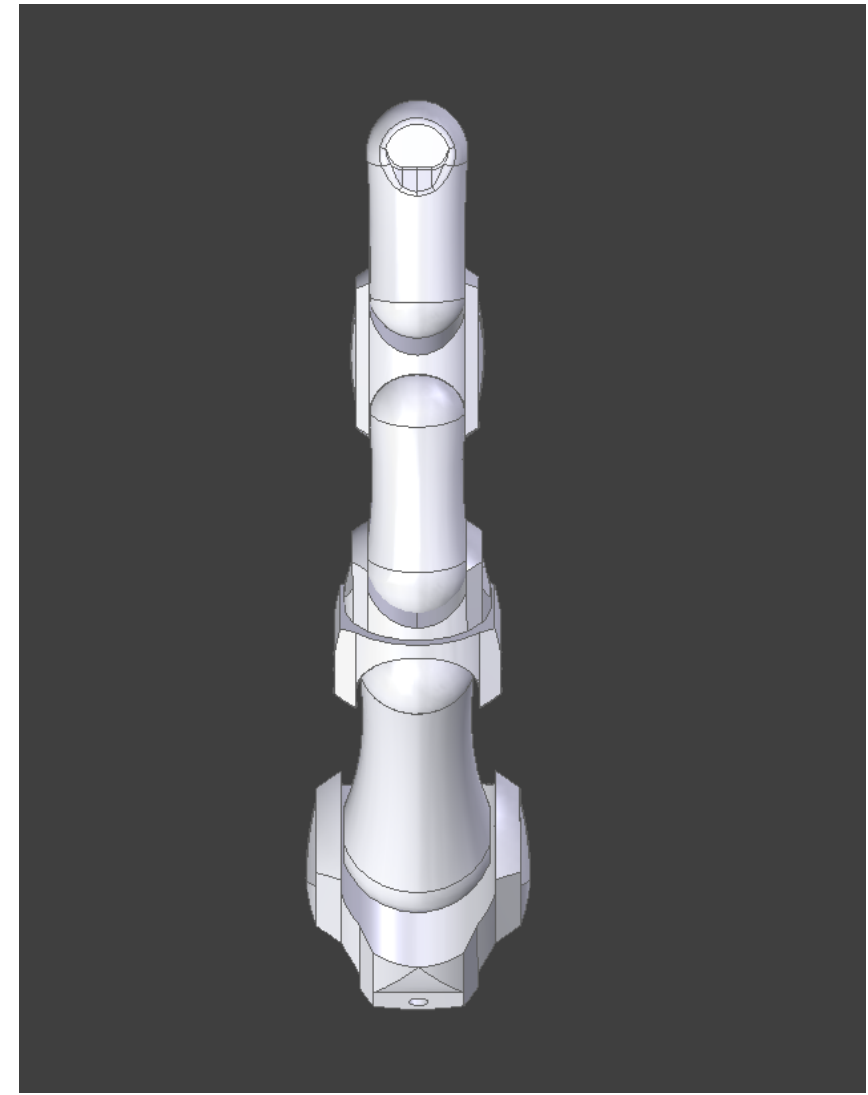


PRODUCED BY AN AUTODESK STUDENT VERSION



AT THE END OF MY PROJECT I WOULD LIKE TO INTRODUCE MY PROTOTYPE HUMAN SECOND FINGER MODEL , WHICH WAS MY FIRST AND AT THE SAME TIME UNSUCCESSFULL APPROACH TO CREATE A 5DOF FINGER AND A 27DOF HUMAN HAND.

CREATED IN THE SIEMENS SOLID EDGE 2020



# PROSTHETIC HAND SZCZYBURA FILIP

## Credits

1. Transfemoral Prosthesis with Polycentric Knee Mechanism: Design, Kinematics, Dynamics and Control Strategy Oleksandr M. Poliakov , Victor B. Lazarev and Olena O. Chepenyuk
2. A Hand Prosthesis with an Under Actuated and Self-Adaptive Finger Mechanism , R. A. R. C. Gopura\*, D. S. V. Bandara
3. Design of a Robotic Hand and Simple EMG Input Controller with a Biologically-Inspired Parallel Actuation System for Prosthetic Applications , Dr. Anthony L. Crawford, Member, IEEE, Jeffrey Molitor, Member, IEEE, Dr. Alba Perez-Gracia Member, IEEE, Dr. Steve C. Chiu, Member, IEEE
4. Chen Chen F., Favetto A., Mousavi M., Ambrosio E.P., Appendino S., Battezzato A., Manfredi D., Pescarmona F., Bona B. (2011). Human Hand: Kinematics, Statics and Dynamics. In: International Conference on Environmental Systems, Portland, Oregon, 17 - 21 Luglio 2011.
5. Inverse Kinematics for Industrial Robots using Conformal Geometric Algebra , A. Kleppe , O. Egeland
6. 1613. Kinematics analysis and optimization of the exoskeleton's knee joint , Shan Jia, Xingsong Wang, Xinliang Lu, Jigang Xu, Yali Han
7. Biomechanics of the human hand, Łukasz Jaworski , Robert Karpiński , Journal of Technology and Exploitation ISSN 2451-148X in Mechanical Engineering Available online at: Vol. 3, no. 1, pp. 28–33, 2017
8. Tailor-Made Hand Exoskeletons at the University of Florence: From Kinematics to Mechatronic Design , Nicola Secciani, Matteo Bianchi, Alessandro Ridolfi, Federica Vannetti, Yary Volpe, Lapo Governi, Massimo Bianchini and Benedetto Allotta
9. 2179. Simulation of the motion of a four bar prosthetic knee mechanism fitted with a magneto-rheological damper , E. M. Attia, M. A. Abd El-Naeem, H. A. El-Gamal, T. H. Awad, K. T. Mohamed
10. Examination of the friction behaviour of artificial HIP joints – brief overview , Volf Leshchynsky\* Instytut Obróbki Plastycznej, ul. Jana Pawła II 14, 61-139 Poznań, Poland
11. A new biarticular actuator design facilitates control of leg function in BioBiped3 , Maziar Ahmad Sharbafi et al 2016 Bioinspir. Biomim.
12. The Role of Morphology of the Thumb in Anthropomorphic Grasping: A Review , Department of Mechanical and Automotive Engineering, Kingston University London, London, United Kingdom, 2 Department of Informatics, King's College London, London, United Kingdom, 3 Dyson School of Design Engineering, Imperial College London, London, United Kingdom
13. How advancements in prosthetic limbs could impact future of sports , Kevin Arnovitz for ESPN
14. <https://www.chemistrylearner.com/alcico.html>
15. <https://www.hortonsoandp.com/how-advanced-prosthetics-are-changing-the-world-of-sports-and-its-athletes/>
16. <https://openbionicslabs.com/obtutorials/ada-v1-assembly>

